Geosphere

Magma hybridization in the middle crust: Possible consequences for deep-crustal magma mixing

Calvin G. Barnes, Carol D. Frost, Øystein Nordgulen and Tore Prestvik

Geosphere 2012;8;518-533
doi: 10.1130/GES00730.1

Notes

Magma hybridization in the middle crust: Possible consequences for deep-crustal magma mixing

Calvin G. Barnes[1], Carol D. Frost[2], Øystein Nordgulen[3], and Tore Prestvik[4]
[1]*Department of Geosciences, Texas Tech University, Lubbock, Texas 79409-1053, USA*
[2]*Department of Geology and Geophysics, University of Wyoming, Laramie, Wyoming 82071, USA*
[3]*Norwegian Geological Survey, N-7491 Trondheim, Norway*
[4]*Department of Geology and Mineral Resources Engineering, University of Trondheim, N-7491 Trondheim, Norway*

ABSTRACT

The 465 Ma Svarthopen pluton in north-central Norway was emplaced under middle-crustal conditions (~700 MPa) into metasedimentary rocks of the Helgeland Nappe Complex. The pluton is characterized by zones of mingling and mixing of gabbro/diorite with peraluminous, garnet-bearing biotite granite. Variation in bulk-rock Sr and Nd isotope ratios are consistent with simple mixing; however, nonuniform enrichment of Zr and the rare earth elements (REEs) suggests that individual magma batches underwent postmixing fractionation. Hybrid intermediate rocks are characterized by Ca-rich garnet. Such garnet is absent in possible mafic end members, and garnet in felsic end members is Ca poor. Evidently, the ferroan, peraluminous hybrid rocks promoted garnet stability, and we interpret these garnets to be igneous in origin. Garnets in the hybrids have low Zr contents, positive light REE slopes, and flat to negative heavy REE slopes with lower REE abundances than in typical igneous garnet. These trace-element data combined with textural evidence suggest that garnet formed near the solidus, after fractionation of zircon, allanite, and possibly xenotime. The Svarthopen pluton is not unique: similar intermediate rocks with Ca-rich garnets crop out adjacent to three other plutons in the region.

Formation of garnet-bearing hybrid rocks in the Svarthopen pluton provides an analog for mixing of peraluminous and ferroan end-member magmas in the deep crust, where such mixing should be widespread, particularly in continental arcs and zones of continental collision. Postmixing fractionation of hybrid magmas could greatly increase the diversity of major- and trace-element abundances yet retain an isotopic signature of mixing. Moreover, formation of garnet-rich hybrids could result in lower-crustal rocks dense enough to delaminate from the arc crust.

INTRODUCTION

Studies of granite origins have traditionally considered crustal sources in terms of specific compositions, for example, metapelitic rocks versus metawackes versus metabasites. Partial melting of each source should, on the basis of theoretical considerations and experimental data, yield characteristic chemical and isotopic features in the resultant magmas (e.g., Clemens et al., 1986; Beard and Lofgren, 1991; Patiño Douce and Johnston, 1991; Skjerlie and Johnston, 1992, 1996; Vielzeuf and Montel, 1994; for a review, see Patiño Douce, 1999). However, modern concepts of arc magmatism (e.g., MASH, Hildreth and Moorbath, 1988; hot zone, Annen et al., 2006; also Dufek and Bergantz, 2005) infer moderate to complete hybridization of mantle-derived basaltic magmas with lower-crustal rocks or with magmas derived from the lower crust. It is evident that where the lower crust is heterogeneous, such hybridization will result in a range of rock compositions that depend on end-member compositions and proportions. Moreover, mixing of dissimilar end members in a hot-zone environment may result in a hybrid in which the mineral assemblage is distinct from either end member. If these hybrid rocks undergo later partial melting, then the resultant magmas will carry the signature of the hybrid rather than of either end member. In such cases, the possibility exists that a range of melt compositions can be generated in the "mixed source," both in terms of bulk composition and isotope ratios.

This study reports examples of midcrustal hybridization in the Norwegian Caledonides. In these examples, partial to complete hybridization of mafic magmas with granitic magmas resulted in relatively Fe-rich hybrids that straddle the metaluminous-peraluminous boundary, contain characteristic Ca-rich garnet, span a range of initial Nd and Sr isotope ratios, and contain incompatible element concentrations higher than either end member. We explore the consequences of this diversity, particularly in terms of the effect of such hybridization on later partial melts of the lower crust.

In addition, we suggest that if mixing at mid-crustal levels can stabilize moderate proportions of garnet, then mixing in the lower crust may result in dense, garnet-rich hybrids. If significant volumes of such hybrids form near the Moho, then the increase in lower-crustal density could result in delamination (e.g., Ducea and Saleeby, 1998; Saleeby et al., 2003; Lee et al., 2006). As these lower-crustal rocks descend into the mantle, they could undergo renewed melting (Xu et al., 2002) and could metasomatize the mantle into which they descend (Lustrino, 2005; Zhang et al., 2010). Delamination could also result in emplacement, and partial melting, of the upper mantle and lower crust at the site of delamination (Collins, 1994; Farmer et al., 2002; Mori et al., 2009; Wells and Hoisch, 2008).

GEOLOGICAL SETTING

The plutonic systems described here intrude rocks of the Helgeland Nappe Complex, the structurally highest nappe complex in the Norwegian Caledonides (Stephens et al., 1985; Stephens and Gee, 1989). The nappe complex is an imbricate nappe stack (Thorsnes and Løseth, 1991) in which the nappes were juxtaposed along E-dipping shear zones prior to ca. 478 Ma (Yoshinobu et al., 2002; Barnes et al., 2007). The nappes consist of either (1) high-grade, commonly migmatitic Neoproterozoic through Ordovician metasedimentary rocks, for which protoliths include sandstones, graywackes, calc-silicate rocks, and marble, or (2) medium- to

Geosphere; April 2012; v. 8; no. 2; p. 518–533; doi:10.1130/GES00730.1; 11 figures; 5 supplemental tables.

high-grade, non-migmatitic metasedimentary rocks, which locally have depositional contacts on ophiolite fragments. Protoliths include mafic, carbonate, and calc-silicate conglomerates; calc-silicate rocks and calcareous sandstone; and marble. Overall, the nappe sequences record deposition on a continental shelf and adjacent seafloor. The Helgeland Nappe Complex is interpreted to have origins along the Laurentian (east Greenland) margin of Iapetus (Stephens and Gee, 1989; Yoshinobu et al., 2002; Roberts, 2003).

Bindal Batholith

Postophiolitic magmatism in the Helgeland Nappe Complex formed the Bindal Batholith, which consists of granitic to gabbroic plutons with ages from ca. 478 to 424 Ma (Birkeland et al., 1993; Nordgulen, 1993; Nordgulen et al., 1993; Yoshinobu et al., 2002; Nissen et al., 2006; Barnes et al., 2007). The oldest plutons crop out in the western part of the batholith and are mainly granitic and peraluminous, reflecting widespread crustal anatexis (Nordgulen et al., 1993; Barnes et al., 2007). Significant contributions of mafic magma into the middle crust occurred locally at ca. 466 Ma (Horta intrusive complex; Gustavson and Prestvik, 1979; Barnes et al., 2005, 2007) and 465 Ma (Svarthopen pluton; Barnes et al., 2007). A magmatic hiatus followed from 465 to ca. 450 Ma (Barnes et al., 2007). Beginning at ca. 450 Ma, granitic through gabbroic magmatism was widespread, especially in the central and western parts of the batholith. In the study area, the gabbroic through quartz monzonitic Velfjord plutons (448–445 Ma; Fig. 1; Barnes et al., 1992, 2004) and the gabbroic to granodioritic Andalshatten pluton (442 Ma; Anderson et al., 2007) are representative of this activity. From 440 to 424 Ma, Bindal magmatism continued to encompass granitic through gabbroic compositions. This activity was even more widespread than from 450 to 440 Ma, encompassing >200 km width of the batholith, with the highest volume of activity in the east (Nordgulen, 1993; Nordgulen et al., 1993; Barnes et al., 2007, 2011). Several of the 440–424 Ma plutons contain ca. 471–462 Ma inherited zircons, which suggests that the ca. 465 Ma magmatism described here was more widespread in the lower crust than surface exposures indicate (Barnes et al., 2007).

In the Velfjord area, scattered outcrops expose rocks that have field characteristics of magma mixing and mingling (herein: hybrids), with net veining, mafic enclaves, and ovoid felsic clots within mafic-intermediate rocks. Such hybrid rocks are best exposed in the Svarthopen pluton and the Hillstadfjellet pluton (in exposures along Heggefjorden near Lundhaug: location 91.10, Fig. 1; Barnes et al., 2002). Other examples of such hybridization are exposed south of the Akset-Drevli pluton (location N155.00; Fig. 1; Barnes et al., 2002) and in scattered locations in the aureole of the Sausfjellet pluton (e.g., location N167.00, Fig. 1). One additional example of hybridization is exposed in the western contact zone of the Hillstadfjellet pluton (location N79.99, Fig. 1), where quartz monzonitic rocks of the pluton are in contact with partly melted host-rock migmatites. Barnes et al. (2002) interpreted partial melting of these migmatites to be related to emplacement of the adjacent pluton, and termed them "contact migmatites."

Field Relations

Svarthopen Pluton

The Svarthopen pluton crops out from the shore of Sørfjorden south and westward to Grøndalsfjellet (Fig. 1; Myrland, 1972; Nordgulen, 1993); it consists of gabbroic and dioritic through granitic rocks. Exposures are generally poor and discontinuous, except for sheets of K-feldspar–megacrystic granite that make bold outcrops along the eastern slope of Grøndalsfjellet. On the basis of exposures near Sørfjord and on Grøndalsfjellet, the predominant mafic rock types are uralitic diorite and gabbro (cf. Myrland, 1972; uralite refers to pyroxenes replaced by pale-green amphibole) that grade into quartz diorite. On the basis of petrographic and geochemical features, we define mafic rocks as having less than 53 wt% SiO_2 and >4 wt% MgO.

Several areas within the pluton are underlain by mingled and mixed mafic and granitic rocks. The best exposure of mixed/mingled rocks is a quarry (Fig. 1) from which most of the field descriptions are taken. In the quarry exposures, mafic rocks range from homogeneous to intricately veined, with veins of medium-grained, garnet-bearing biotite granite (Fig. 2A). In some locations, the mafic rocks have the appearance of magmatic "pillows" (Fig. 2B) that are back-veined by the granite; in other locations the mafic rocks are net-veined with variable degrees of hybridization (Fig. 2C); and in others, mafic/intermediate rocks comprise biotite-rich layers within granitic sheets and dikes. Parts of the pluton underwent high-temperature deformation, which resulted in a foliation defined by elongate mafic enclaves and oriented biotite and feldspar (Fig. 2D).

In this work, intermediate rocks are identified as ones with variable values of color index between the mafic (gabbro to quartz diorite) rocks and true granites. These intermediate rocks range from quartz diorite through tonalite to granodiorite, and they range in SiO_2 content from 53 to 70 wt% (see following). Many of these samples contain garnet crystals as much as 5 mm in diameter. These intermediate rocks were interpreted in the field to be hybrids on the basis of their heterogeneity (Figs. 2C–2F), local presence of large feldspar crystals similar to those in the granites, and the presence of garnet, which was initially interpreted to be inherited from the granitic magmas. The modal proportion of garnet reaches ~10% in rocks with intermediate color index (Fig. 2E). Some garnet crystals are located on the contact between the two rock types and some are surrounded by a thin leucocratic rind (Figs. 2E and 2F).

Hillstadfjellet Pluton

General descriptions of the Hillstadfjellet pluton were presented by Barnes et al. (1992, 2002), who subdivided the pluton into two stages. The older stage 1 consists of gabbro and diorite in which pyroxene is commonly uralitized and primary amphibole is poikilitic. These rocks are petrographically similar to the gabbro, diorite, and quartz diorite of the Svarthopen pluton. The age of stage 1 has not been determined, but it is intruded by 444.8 Ma diorite to quartz monzonite of stage 2 (Barnes et al., 1992; Yoshinobu et al., 2002). The intrusive contact between the two stages is characterized by intrusion breccia, with centimeter- to meter-scale blocks of stage 1 rocks enclosed in stage 2 rocks. Garnet-bearing quartz diorite and tonalite crop out along the eastern side of the Hillstadfjellet pluton near Lundhaug (Fig. 1; Barnes et al., 1992), where they are associated with stage 1 rocks.

Hillstadfjellet, Akset-Drevli, and Sausfjellet Aureoles

In the western aureole of the Hillstadfjellet pluton, stage 2 rocks are mingled with contact migmatites in the aureole (location N79.99, Fig. 1). In the southern aureole of the Akset-Drevli pluton, a dioritic dike mingled with leucosome magma from a diatexitic migmatite to produce a garnet biotite tonalite (Fig. 3H *in* Barnes et al., 2002). Garnet is lacking in both the diorite and the migmatite, but it is present in the hybrid. In the western aureole of the Sausfjellet pluton, a garnet amphibole quartz diorite crops out (sample N167.00, Fig. 1). Although the field relationships of this latter sample are unclear, it is included here because the assemblage is similar to other garnet-bearing hybrids.

Geochronology

Zircons from a granitic dike in the Svarthopen quarry (N03.05) were dated by laser-ablation–inductively coupled plasma–mass spectrometry (LA-ICP-MS; Barnes et al., 2007). The sample yielded a range of concordant dates from 454

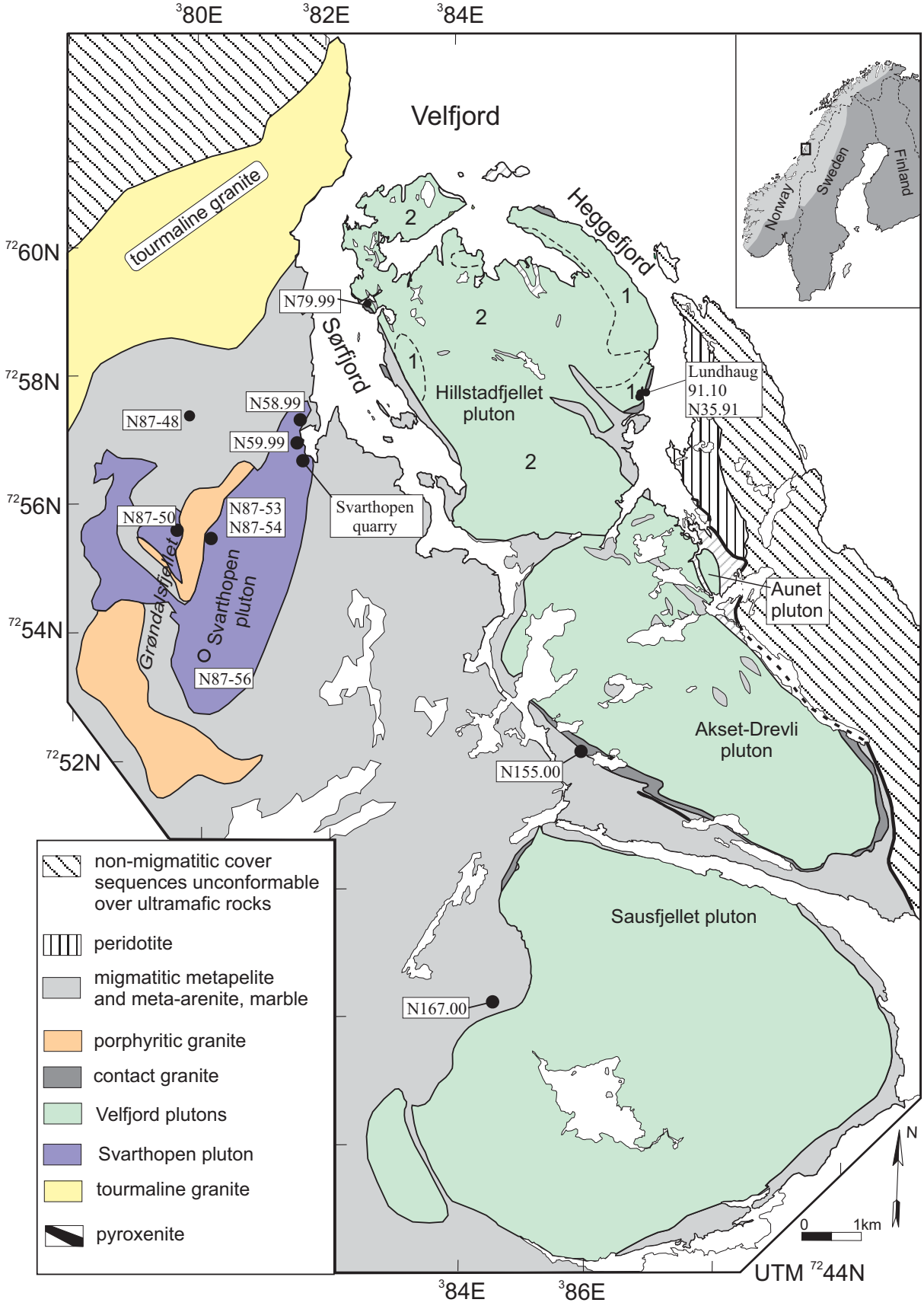

Figure 1. Simplified geologic map of the Velfjord area, after Barnes et al. (2002); UTM grid ED50, zone 33. Inset shows location.

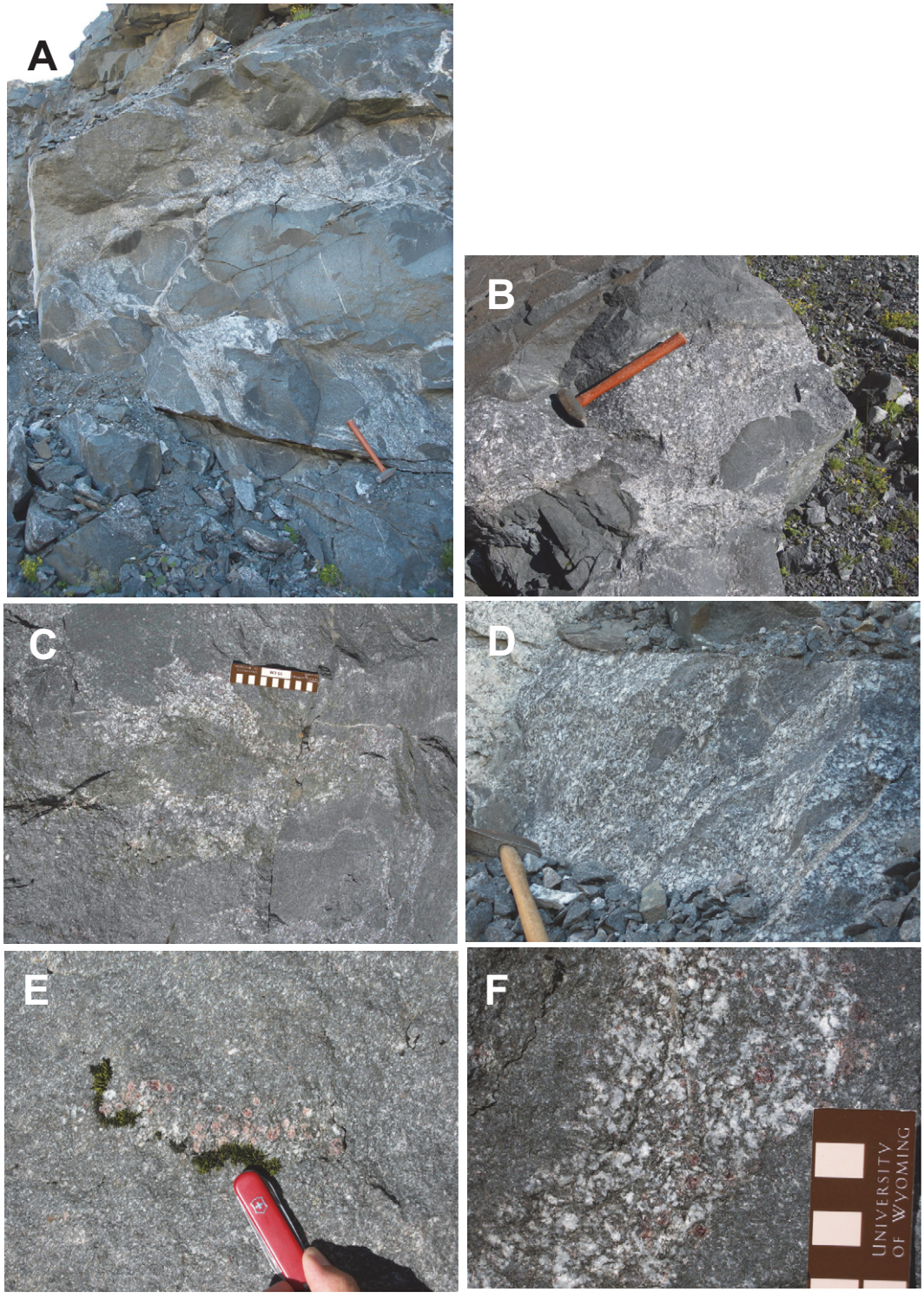

Figure 2. Outcrop photographs of the Svarthopen quarry. (A) Mingled K-feldspar–phyric granite and quartz dioritic enclaves. (B) Mingled granite with quartz dioritic–tonalitic enclaves back-veined by the host granite. (C) Net-veined hybrid tonalitic enclaves. Units on scale are cm. (D) Deformed (stretched?) tonalitic enclaves in foliated granitic host. (E) Cluster of garnets in tonalitic hybrid. (F) A pod of garnet-bearing granite enclosed in garnet-bearing tonalitic hybrid.

to 503 Ma. A cluster of the youngest dates was interpreted to represent the magmatic age, at 465.0 ± 1.5 Ma, with older ages interpreted as inheritance. Stage 2 of the Hillstadfjellet pluton was dated at 444.8 ± 2.2 Ma using the multicrystal thermal ionization mass spectrometry (TIMS) method (Yoshinobu et al., 2002).

PETROGRAPHY

Svarthopen and Hillstadfjellet Plutons

Dioritic and gabbroic rocks from the Svarthopen pluton that were collected more than 100 m from zones of hybridization typically have hypidiomorphic granular to diabasic textures (Fig. 3A) that are variably deformed into protoclastic assemblages. The primary igneous assemblage is plagioclase, augite, Ca-amphibole, and quartz ± biotite, with accessory apatite, Fe-Ti oxides, and zircon. Plagioclase is lath shaped and is normally zoned, with anhedral

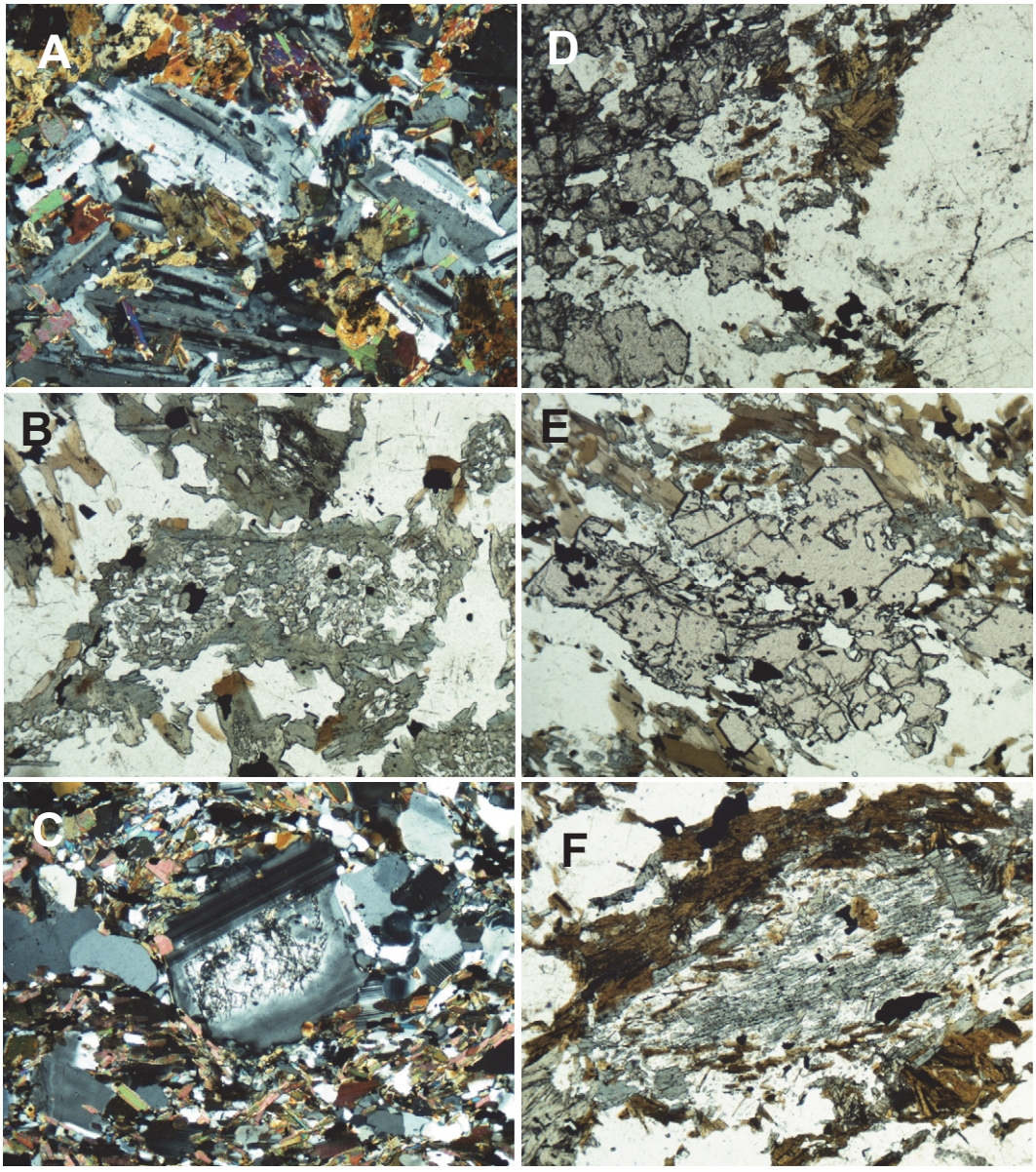

Figure 3. Photomicrographs of rocks from the Svarthopen intrusion. The length dimension of all images is 2 mm. (A) Relict diabasic texture in quartz diorite sample N58.99. Pyroxene replaced by hornblende. (B) Relict pyroxene (augite?) replaced by granular hornblende, plagioclase, and quartz, from quartz diorite sample N59.99. Primary, olive-green hornblende partly rims relict pyroxene. (C) Plagioclase porphyroclast with ~An_{70} core and An_{40} rim in hybrid tonalite N57.99A. (D) Ragged garnet (left) and plagioclase porphyroclast (right) separated by biotite, plagioclase, and quartz in tonalitic hybrid N132.00. (E) Sheared garnet with ragged and idiomorphic boundaries, tonalitic hybrid sample N57.99A. (F) Fine-grained cluster of elongate, blue-green amphibole, quartz, and plagioclase (relict augite?) partly surrounded by biotite in tonalitic hybrid sample N132.00.

cores as calcic as An_{75} and broad, weakly zoned rims ~An_{40}. Sparse plagioclase phenocrysts reach three mm in length; groundmass crystals average 0.5 mm long. Many crystals are slightly bent and show deformation twinning and recrystallization along grain boundaries. The primary pyroxene is generally totally replaced, either by actinolitic amphibole or more commonly by clusters and sheaves of pale-green amphibole, quartz, ilmenite, titanite, and biotite. Both types of replacement assemblages are partly surrounded by medium-grained olive- to pale-green amphibole (Fig. 3B). Some samples contain poikilitic olive amphibole and sparse poikilitic biotite. Accessory apatite occurs as equant, euhedral to anhedral crystals as much as 1 mm long and also as acicular crystals. In one sample, skeletal (?) clusters of acicular apatite inclusions in poikilitic amphibole reach 1.5 mm in length. We interpret such acicular and skeletal apatite as having formed in undercooled magma (e.g., Vernon, 1983), not in the solid state. In fact, trains of thin apatite inclusions in plagioclase indicate the original presence of acicular apatite that was broken during high-temperature deformation of the host crystals. Accessory zircon is equant and euhedral and reaches 0.4 mm in maximum dimension. Ilmenite varies widely in habit, from elongate crystals that reach 1 mm in length to subequant inclusions in the mafic silicates and plagioclase.

Granitic dikes for which field relationships indicate coeval emplacement with the diorites are typically foliated, porphyroclastic garnet biotite granite. Porphyroclasts consist of K-feldspar, plagioclase, and sparse garnet and biotite. Plagioclase is normally zoned, with ~An_{40} cores and ~An_{25} rims, and some crystals display faint oscillatory zoning. Garnet reaches 1 cm in diameter, and some crystals are rimmed by plagioclase + quartz + muscovite; others are cut by veins of muscovite + biotite + plagioclase. Garnet in the granitic rocks encloses acicular apatite. The foliation in these rocks is defined by biotite and by discontinuous zones of fine-grained feldspars and quartz. Some biotite is deformed around garnet porphyroclasts, whereas some abuts the garnet in pressure shadows. Accessory phases are apatite, zircon, and ilmenite, with scant secondary epidote and

muscovite. Intergranular titanite may be a late primary phase or deuteric.

Svarthopen samples identified as hybrid rocks in the field are mainly quartz diorite and tonalite, with lesser amounts of granodiorite. Their original texture (hypidiomorphic granular?) was modified by ductile deformation, leaving porphyroclasts of plagioclase, garnet, biotite, and quartz set in a fine- to medium-grained matrix of plagioclase, quartz, reddish brown biotite, and pale-green amphibole. Plagioclase porphyroclasts are blocky, some are broken, and many have undergone subgrain development to form aggregates of equant plagioclase. The plagioclase is zoned (Fig. 3C), with calcic to intermediate cores ($An_{74–45}$) and broad rims ($An_{49–27}$, typically An_{40}). Inclusions of acicular apatite are common in plagioclase. Quartz porphyroclasts have undergone subgrain development. Garnet ranges from equant to "flattened" or elongate, and most grains have ragged boundaries with a few well-formed faces (Figs. 3D and 3E). The garnet shown in Figure 3E is sheared, presumably by the ductile deformation that deformed feldspars in these rocks. Inclusions in garnet are quartz, plagioclase, ilmenite, apatite, and biotite. The abundance of ilmenite inclusions is variable, and where it is in greatest abundance, the grains are oriented parallel to cleavage in adjacent biotite. Small, acicular apatite is present in parts of the garnet with small proportions of ilmenite. Some apatite crystals are oriented parallel to garnet grain boundaries, whereas others are oriented at high angles to grain boundaries.

The proportions of matrix amphibole and biotite vary from sample to sample. The amphibole is blue-green to pale olive and is generally intergrown with biotite, quartz, and plagioclase; however, some samples contain prismatic and intergranular amphibole. Many samples contain 1–2-mm-scale intergrowths of fine-grained amphibole, biotite, plagioclase, and quartz with shapes that suggest replacement of pyroxene or amphibole phenocrysts (Fig. 3F). In addition to acicular apatite, these rocks contain robust, rounded, intergranular apatite. Zircon occurs primarily as elongate prisms, with aspect ratios of as much as 10:1 and lengths to ~270 µm. Some samples contain tourmaline, and all contain interstitial metamict allanite. Sparse secondary minerals are titanite, chlorite, and rare clinozoisite.

Hybrid samples from the eastern Hillstadfjellet pluton are similar to those from Svarthopen, although in some samples, garnet is primarily equant and subidiomorphic. In these rocks, acicular apatite reaches 1 mm in length, and some acicular crystals cross plagioclase-garnet grain boundaries. Zircon varies from stubby euhedral grains to elongate prisms that reach 0.7 mm in length.

Hillstadfjellet, Akset-Drevli, and Sausfjellet Aureoles

Garnet-bearing rocks that resulted from diorite-migmatite hybridization in the western aureole of the Hillstadfjellet pluton are medium-grained, protoclastic, garnet amphibole biotite quartz diorite. Plagioclase and amphibole porphyroclasts are set in a medium- to fine-grained matrix of recrystallized plagioclase, quartz, biotite, amphibole, apatite, and opaque minerals. Blocky plagioclase contains acicular apatite inclusions. Garnet shows idiomorphic contacts against biotite but ragged contacts against other phases; some garnet poikilitically encloses plagioclase and quartz. Garnet also contains inclusions of ilmenite and acicular apatite. Radioactive accessory phases are common inclusions in biotite.

The hybrid tonalite from the Akset-Drevli aureole contains equant, subidiomorphic garnet and biotite; amphibole is absent. Plagioclase in the Akset-Drevli hybrid is nearly uniform in composition at An_{37}.

The hybrid sample collected in the Sausfjellet aureole (N167.00) is medium-grained, hypidiomorphic granular garnet biotite amphibole quartz diorite. Relict pyroxene is variably replaced by prismatic to sheaf-like cummingtonite, and the cummingtonite is rimmed by or intergrown with medium-olive– to blue-green amphibole. Some amphibole overgrowths are euhedral and are surrounded by biotite, and some isolated euhedral/subhedral green amphibole grains are present. Garnet habits are similar to those in the Svarthopen hybrids, and garnet encloses ilmenite, biotite, and quartz. Reddish-brown biotite ranges from idiomorphic to poikilitic. Plagioclase crystals are slightly elongate to blocky, with seriate distribution to 5 mm long; plagioclase is zoned from An_{72} cores to An_{42} rims. Accessory apatite occurs as equant, grains to 0.3 mm diameter. Other accessory minerals are ilmenite, zircon, and allanite.

Analytical Methods

Mineral compositions (Supplemental Tables 1[1] and 2[2] were analyzed on an automated JEOL 8900 Superprobe at the University of Wyoming. Nominal instrument conditions were 15 kV accelerating potential and 10–20 nA beam current. Standards were natural and synthetic silicates and oxides; data were reduced using ZAF corrections. Trace-element compositions of minerals (Supplemental Table 3[3]) were analyzed by LA-ICP-MS at the Australian National University (193 nm Excimer laser and Agilent 7500S ICP-MS) and Texas Tech University (213 nm solid-state laser and Agilent 7500cs ICP-MS). Spot sizes were 30–40 µm, and NIST 612 glass was the calibration standard. Each spectrum included analysis for Ti, Fe, and P in order to identify and exclude analyses contaminated by inclusions of apatite and/or Fe-Ti oxides. Bulk-rock compositions (Supplemental Table 4[4]) were determined by X-ray fluorescence and inductively coupled plasma–atomic emission spectroscopy (AES) (major and trace elements) and ICP-MS (trace elements; see Supplemental Table 4 [see footnote 4] for details). Analytical methods for Sr and Nd isotopes are given as footnotes to Supplemental Table 5.[5]

Garnet Compositions

Garnet from the Svarthopen granites is essentially unzoned and has compositions near $Gr_3Py_{5–7}Alm_{77–80}Sp_{10–13}$ (Supplemental Table 1 [see footnote 1]). Figure 4A shows that the grossular component is nearly constant over a range of Fe/(Fe + Mg) values and that garnet from the Svarthopen granite is compositionally similar to garnets from regional high-grade migmatitic rocks (data from Barnes and Prestvik, 2000; Barnes et al., 2002). In contrast, garnet from the hybrid quartz diorite and tonalites is commonly more calcic (Supplemental Table 1 [see footnote 1]; Fig. 4A), with average grossular contents from 16% to 18%. In sample N55.99c from the Svarthopen quarry, the interiors of garnet crystals have low grossular contents identical to garnet in the granites, but the garnet rims have grossular contents of ~12% (Fig. 4A).

[1]Supplemental Table 1. Excel file of representative and average garnet compositions. If you are viewing the PDF of this paper or reading it offline, please visit http://dx.doi.org/10.1130/GES00730.S1 or the full-text article on www.gsapubs.org to view Supplemental Table 1.

[2]Supplemental Table 2. Excel file of representative amphibole compositions. If you are viewing the PDF of this paper or reading it offline, please visit http://dx.doi.org/10.1130/GES00730.S2 or the full-text article on www.gsapubs.org to view Supplemental Table 2.

[3]Supplemental Table 3. Excel file of representative garnet trace-element concentrations (ppm). If you are viewing the PDF of this paper or reading it offline, please visit http://dx.doi.org/10.1130/GES00730.S3 or the full-text article on www.gsapubs.org to view Supplemental Table 3.

[4]Supplemental Table 4. Excel file of major- and trace-element compositions of bulk-rock samples. If you are viewing the PDF of this paper or reading it offline, please visit http://dx.doi.org/10.1130/GES00730.S4 or the full-text article on www.gsapubs.org to view Supplemental Table 4.

[5]Supplemental Table 5. Excel file of Nd and Sr isotopic data for the Svarthopen pluton. If you are viewing the PDF of this paper or reading it offline, please visit http://dx.doi.org/10.1130/GES00730.S5 or the full-text article on www.gsapubs.org to view Supplemental Table 5.

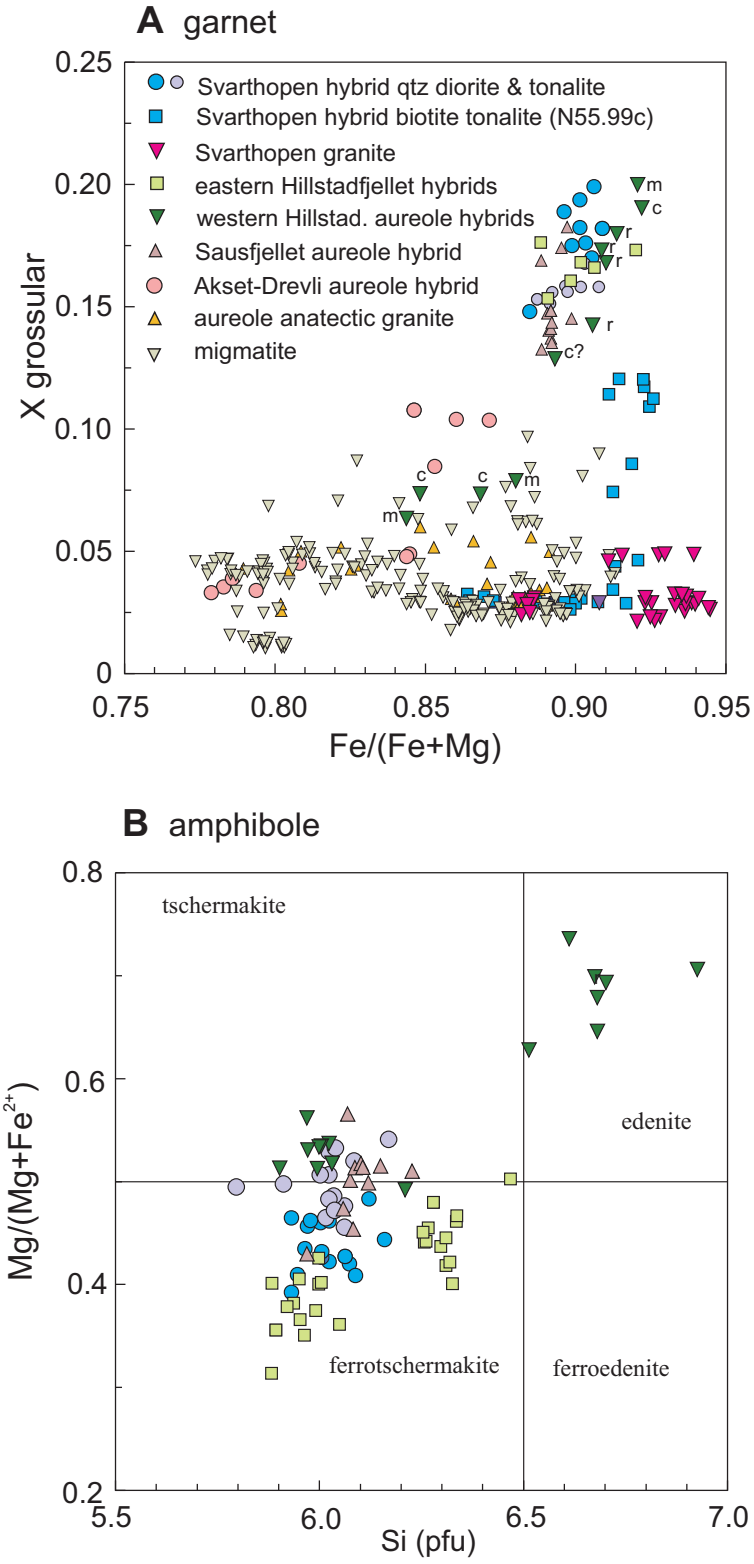

Figure 4. (A) Grossular contents plotted versus Fe/(Fe + Mg) in garnets from the Svarthopen and related hybrids and from regional migmatites and contact granites (cf. Barnes et al., 2002). For the western Hillstadfjellet hybrid (sample N30.91), core (c), mantle (m), and rim (r) analyses are labeled. (B) Classification of amphibole from hybrid Svarthopen (N59.99A, N132.00) and Hillstadfjellet (91.10) tonalites.

In other words, Ca-rich garnets are present in rocks identified as hybrids in the field, whereas Ca-poor garnets characterize the granitic rocks and regional metamorphic rocks with pelitic compositions.

Garnets in hybrid rocks from the eastern Hillstadfjellet pluton are similar to those from Svarthopen hybrids (Fig. 4A). In contrast, garnets from the western aureole of the Hillstadfjellet pluton (hybridized with migmatite) have both Ca-rich and Ca-poor zones; most Ca-poor compositions are from garnet cores and mantles (Fig. 4A). Garnets from the hybrid in the aureole of the Akset-Drevli pluton (N155.00A) are similar in composition to garnets from regional metamorphic rocks, but some analyses show intermediate grossular contents, similar to sample N55.99c (Fig. 4A). Garnet from the Sausfjellet aureole overlaps the compositional range of garnets from Svarthopen hybrids.

The rare earth element (REE) patterns of garnet from granitic rocks have steep, positive slopes with large, negative Eu anomalies (Figs. 5A and 5B; see Supplemental Table 3 [see footnote 3]). Garnets from biotite tonalite sample N55.99c have REE patterns similar to those from the granitic rocks (Fig. 5C). In contrast, REE patterns for garnet in hybrid sample N57.99A are of two types: those with steep positive slopes and deep Eu anomalies (representing garnet cores), and those with steep light REE (LREE) slopes, flat heavy REE (HREE) slopes, and no Eu anomaly (representing crystal mantles and rims). Garnets from a second Svarthopen tonalite and a hybrid quartz diorite from the eastern Hillstadfjellet pluton (Figs. 5E and 5F) also have flat HREE patterns, and both have slight positive Eu anomalies. These features are exaggerated in garnet from the Sausfjellet aureole hybrid (Fig. 5G). Garnet from the diorite-migmatite hybrid in the western Hillstadfjellet aureole is distinct relative to all other samples, with steep LREE slopes, variable negative Eu anomalies, high normalized Tb and Dy concentrations, and then decreasing abundances among the remaining HREEs (Fig. 5H). A more subtle feature in these data is the fact that the LREE abundances in many of the garnets from hybrid rocks are lower than in garnets from the granites. For example, garnet from granitic rocks contains 1–2× chondritic abundances of Nd, whereas garnet from the hybrid rocks contains <0.8× chondritic abundances.

Another indication of the differences in garnet trace-element abundances is shown in Figure 6, which plots Zr and Y concentrations. Garnets with low grossular contents, overall steep REE patterns, and negative Eu anomalies have widely variable Zr and Y concentrations, with Zr as high as 65 ppm and Y as high

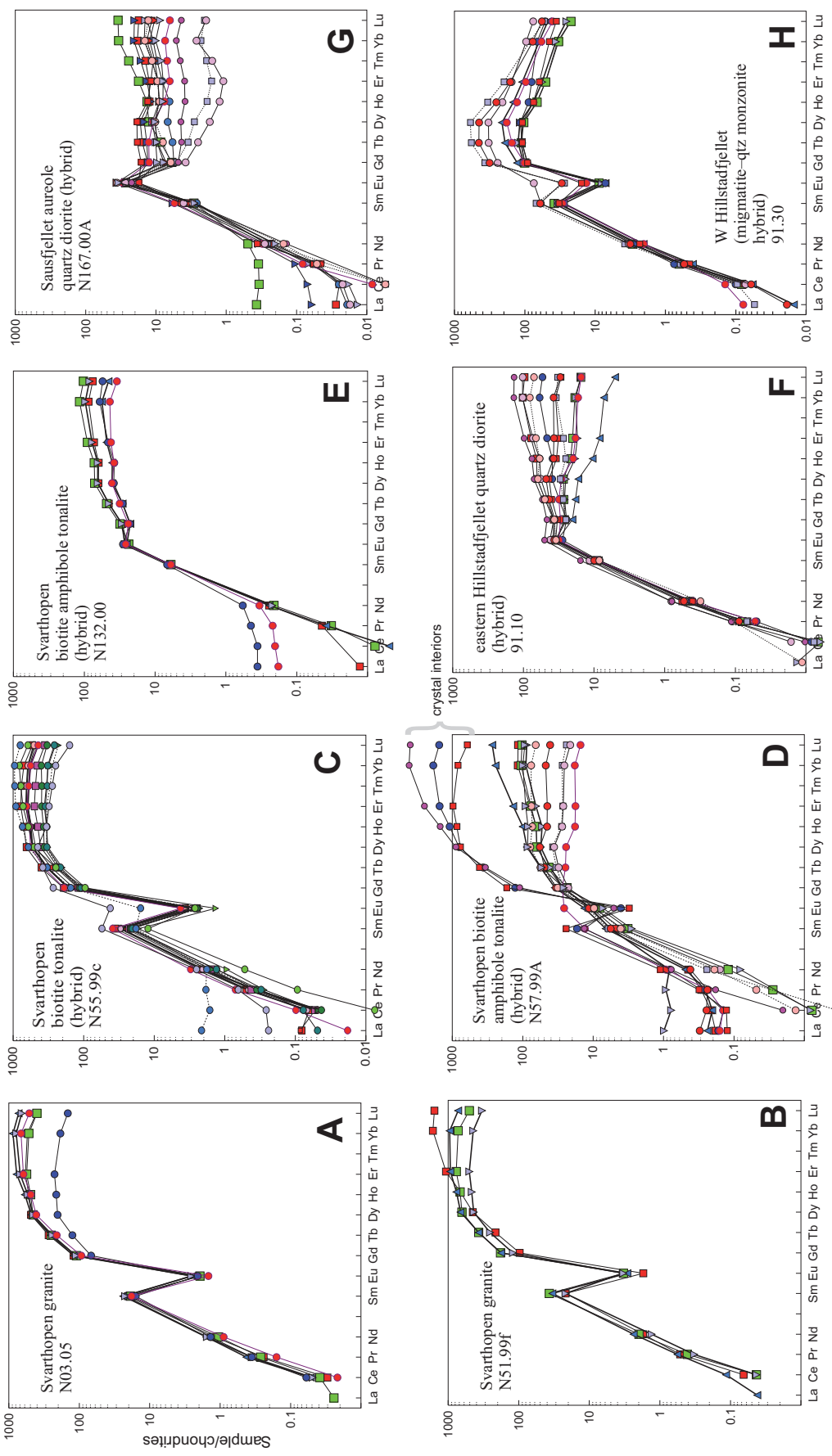

Figure 5. Rare earth element (REE) patterns of garnet. See text for discussion.

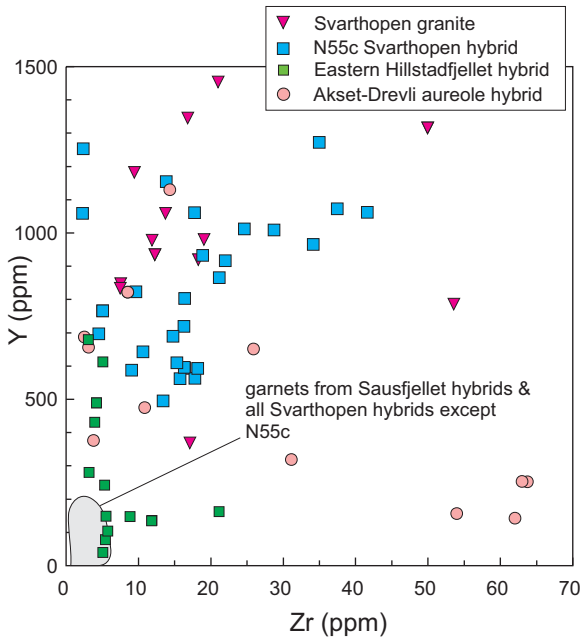

Figure 6. Zr and Y contents of garnet from hybrid samples and related granites.

as 2500 ppm. Most Ca-rich garnets have low Y contents, consistent with their comparatively low HREE abundances, and all Ca-rich garnets have <10 ppm Zr (Fig. 6).

Amphibole Compositions

Calcic amphibole in the hybrid rocks from Svarthopen, the eastern part of the Hillstadfjellet pluton, and the Sausfjellet aureole are aluminous, with 1.7–2.2 Al per formula unit (Supplemental Table 2 [see footnote 2]). The values of $Mg/(Mg + Fe^{2+})$ range from 0.32 to 0.57, so the amphiboles are classified as ferrotschermakite and tschermakite (Fig. 4B; classification of Leake et al., 1997). Calcic amphibole from the diorite-migmatite hybrid in the western aureole of the Hillstadfjellet pluton is also aluminous, and the majority of analyses plot in the edenite field, but a few are tschermakite and similar to amphibole from the Svarthopen hybrid samples.

Thermobarometry

The garnet + amphibole + plagioclase assemblage in hybrid rocks permits use of the garnet-hornblende barometer of Kohn and Spear (1990). The garnet + hornblende assemblage is in textural equilibrium with plagioclase with a composition of An_{40}. For four samples, the Kohn and Spear (1990) algorithms result in pressure estimates from 600 to 700 MPa and temperature estimates from 500 to 550 °C.

Ti-in-zircon thermometry (Watson et al., 2006; Ferry and Watson, 2007) was applied to zircons from Svarthopen granite sample N03.05 (data from Barnes et al., 2007). The average temperature determined from concordant zircons that were used to calculate the magmatic age is 732 ± 36 °C. In contrast, the zircon saturation temperatures for felsic rocks in the Svarthopen pluton are ≥850 °C. Although it is possible that the high zircon saturation temperatures are the result of inherited zircon, concentrations of other trace elements in the hybrid rocks suggest alternative explanations, which are presented in the Discussion.

GEOCHEMISTRY

Samples from the Svarthopen intrusion range in SiO_2 concentration from 48%–74% (Supplemental Table 4 [see footnote 4]; Fig. 7). Among samples collected near the Svarthopen quarry, those that lack textural evidence of hybridization (the mafic rocks of the pluton; see previous) have SiO_2 between 48% and 53% and MgO from 5 to 6 wt% (Fig. 7A). Rocks identified as hybrids contain 53%–66% SiO_2 and 1.3%–3.7% MgO. Granitic rocks have ≥70% SiO_2 and <1% MgO. The garnet-bearing Hillstadfjellet hybrids have similar bulk compositions. Contents of CaO decrease smoothly with increasing SiO_2, with the Hillstadfjellet garnet-bearing hybrids being slightly more calcic than Svarthopen hybrids at similar silica contents (Fig. 7B).

The classification of Frost and Frost (2008) shows that mafic samples from the Svarthopen area are magnesian, but that with increasing SiO_2 the hybrid and granitic rocks plot along the boundary separating magnesian and ferroan fields (Fig. 7C). Several samples from Grøndalsfjellet plot in the ferroan field. The modified alkali-lime index (Fig. 7D; Frost et al., 2001) shows that all samples plot within the calc-alkaline and alkali-calcic fields. The alumina saturation index (ASI; Fig. 7E) varies from values <1 for the mafic rocks to values >1 for the Svarthopen hybrids and granitic rocks. Several of these samples are strongly peraluminous, with ASI >1.1. Most Hillstadfjellet hybrids plot in the metaluminous field.

Some trace-element abundances plot along smooth trends with increasing SiO_2. Figure 8A shows variation of Sr, which decreases from ~400 ppm for the quartz diorites to <100 ppm for the granites. The eastern Hillstadfjellet hybrids plot along this trend, but the western Hillstadfjellet hybrid rocks (migmatite–quartz monzonite hybrids) have much higher Sr contents (>950 ppm; Fig. 8A). This discrepancy may be explained by comparison with Sr contents of the rest of the Hillstadfjellet pluton, shown as fields in Figure 8A. Stage 1 Hillstadfjellet samples plot in two fields, one of which is near the low-SiO_2 extension of the Svarthopen trend. In contrast, stage 2 Hillstadfjellet samples range from 1400 ppm to ~300 ppm Sr, i.e., values much higher than in the Svarthopen samples. It is probable that the eastern, garnet-bearing Hillstadfjellet hybrids had mafic end members similar to low-Sr stage 1 samples of the Hillstadfjellet pluton, whereas the Sr-rich hybrids from the western Hillstadfjellet pluton had end members similar to stage 2 Hillstadfjellet magmas.

The concentrations of Ba, Y, and Zr (Figs. 8B–8D) increase with increasing SiO_2 from mafic through hybrid tonalite compositions and then decrease among the granitic samples. Variation of all three elements, and particularly Zr, is considerably more scattered than for Sr.

The REE patterns for Svarthopen and Hillstadfjellet samples are all LREE enriched (Fig. 9). Svarthopen mafic rocks have small negative Eu anomalies. The granitic rocks from the Svarthopen pluton have REE contents similar to those of the mafic rocks, but they have deeper Eu anomalies. In contrast, the REE contents of the hybrid rocks extend to significantly higher concentrations, and the slopes of the HREE part of the patterns are flatter than for the mafic rocks and granites.

Sr and Nd Isotopes

Figure 10 shows the range of Sr and Nd isotope ratios for the Svarthopen pluton (Supplemental Table 5 [see footnote 5]; calculated at 465 Ma) and the nearby Velfjord plutons (calculated at 448 Ma; Nordgulen and Sundvoll,

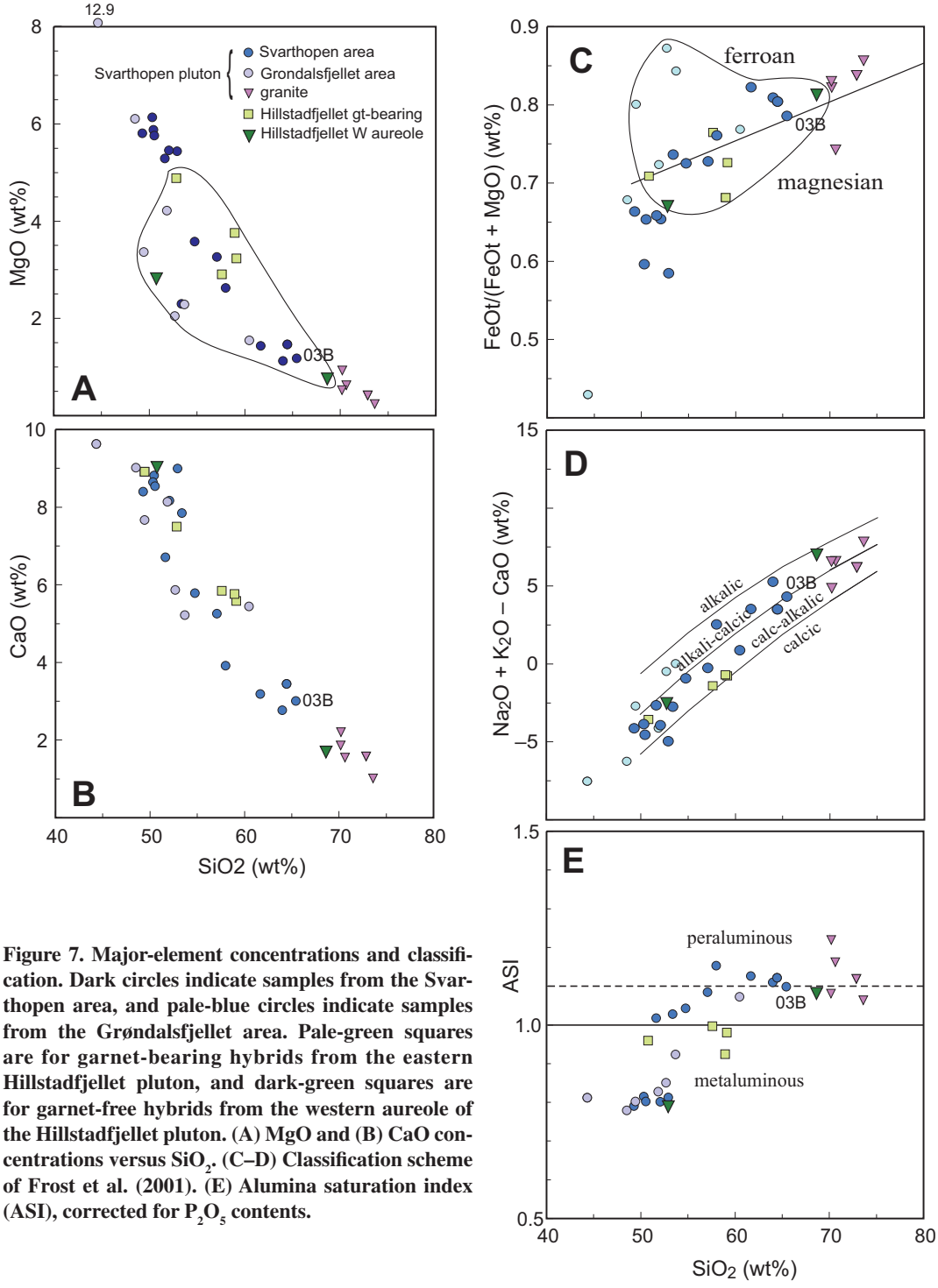

Figure 7. Major-element concentrations and classification. Dark circles indicate samples from the Svarthopen area, and pale-blue circles indicate samples from the Grøndalsfjellet area. Pale-green squares are for garnet-bearing hybrids from the eastern Hillstadfjellet pluton, and dark-green squares are for garnet-free hybrids from the western aureole of the Hillstadfjellet pluton. (A) MgO and (B) CaO concentrations versus SiO_2. (C–D) Classification scheme of Frost et al. (2001). (E) Alumina saturation index (ASI), corrected for P_2O_5 contents.

1992; Barnes et al., 2002; Supplemental Table 5 [see footnote 5]). Compared to the Velfjord plutons, even the most mafic Svarthopen rocks have lower ε_{Nd} (<–3). In contrast, the granitic dikes and sheets in the Svarthopen pluton are isotopically similar to anatectic granites in the aureoles of the Velfjord plutons (e.g., Barnes et al., 2002; Fig. 10). Initial $^{87}Sr/^{86}Sr$ values are positively correlated with SiO_2 and K_2O and show weak negative correlation with CaO, MgO, Sr, and Mg/(Mg + Fe). In contrast, Zr, Y, and LREE contents are essentially uncorrelated with initial $^{87}Sr/^{86}Sr$.

Depleted mantle model ages for samples from the Svarthopen pluton range from 1.8 to 1.5 Ga (Supplemental Table 5 [see footnote 5]), with the oldest value belonging to a granitic dike. These values are similar to those calculated for granitic rocks associated with regional migmatization (2.0–1.2 Ga; Barnes et al., 2002) and are older than those calculated for the dioritic to monzonitic Sausfjellet pluton (1.2–0.8 Ga; data from Barnes et al., 2004). The model ages are therefore consistent with an origin of the granitic

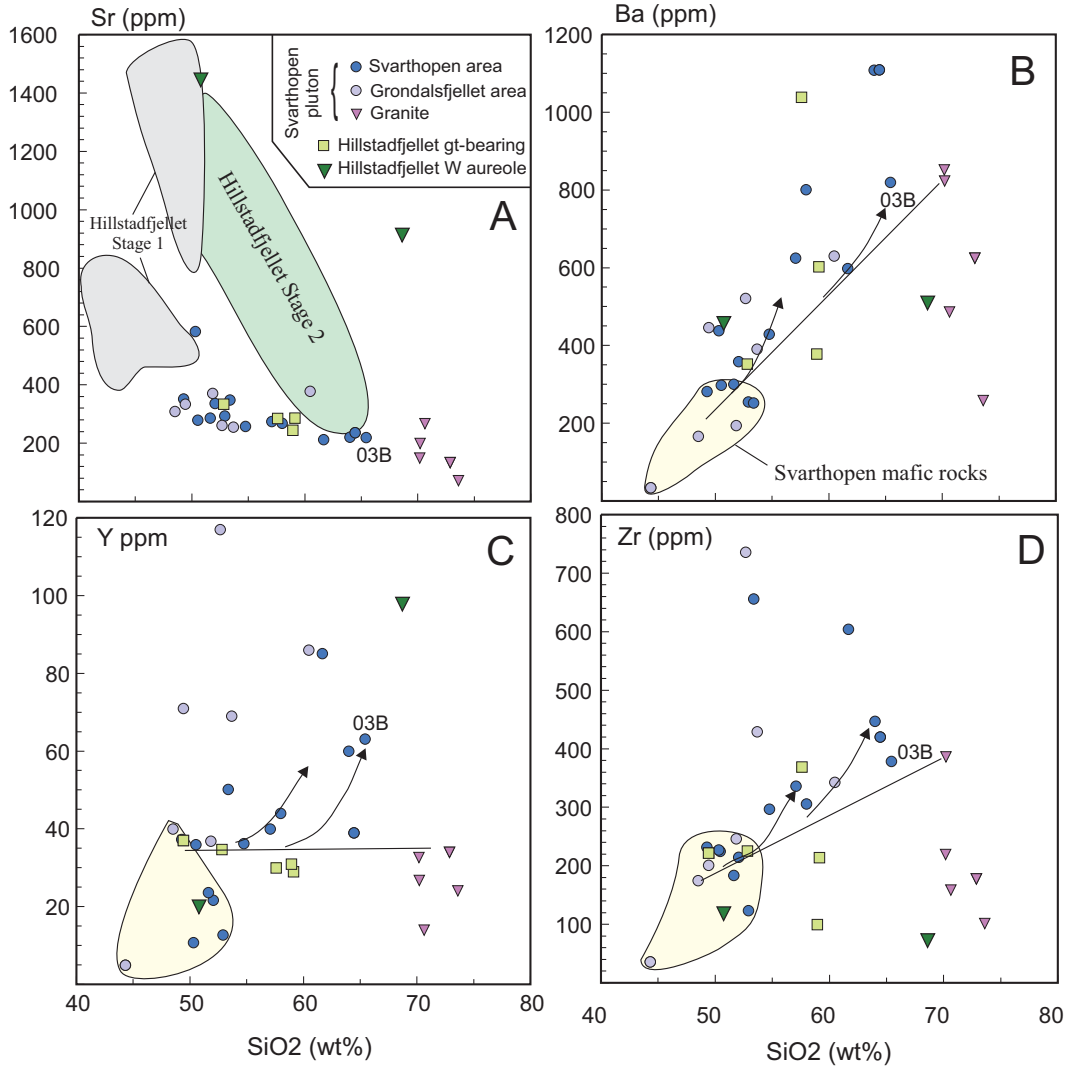

Figure 8. Trace-element concentrations (ppm) plotted against SiO_2. (A) Sr concentrations in all but one Svarthopen sample are <400 ppm, as are Sr concentrations in hybrids from the eastern Hillstadfjellet pluton. Hybrids from the western Hillstadfjellet pluton have >900 ppm Sr. The shaded fields represent the range of compositions of the Hillstadfjellet pluton: gray—stage 1, green—stage 2. (B) Ba concentrations. (C) Y concentrations. (D) Zr concentrations. In panels B–D, the straight line represents a mixing line between dioritic and granitic end members. The curves are suggested compositional trends followed by hybrid magmas that differentiated after magma mixing.

magmas in the Svarthopen pluton as partial melts of metamorphic rocks similar to those exposed in the Helgeland Nappe Complex.

DISCUSSION

Field evidence indicates that much of the Svarthopen pluton is of hybrid origin, caused by mixing/mingling of mafic, mainly dioritic magmas with granitic magmas. A mixing origin is also supported by the abrupt core-rim boundaries in plagioclase (Fig. 3) and smooth variation of Sr and Nd isotope values that can be modeled with a simple mixing relationship (Fig. 10). One of the characteristic features of intermediate, hybrid rocks in the Svarthopen pluton is the presence of Ca-rich garnet. In contrast, garnet is absent in mafic rocks in the Svarthopen pluton and also the nearby Velfjord plutons, and garnet in the granitic rocks and migmatites of the region is Ca poor. Ca-rich garnet also characterizes hybrids from the eastern part of the Hillstadfjellet pluton and from the aureoles of the Velfjord plutons.

The presence of garnet in peraluminous granites, including many in the Helgeland Nappe Complex, is commonplace (e.g., Miller and Stoddard, 1981; Allan and Clarke, 1981; Zen, 1988; Erdmann et al., 2009; Lackey et al., 2011). These studies and many others have shown that such garnets are typically almandine rich, as are those studied here. However, garnets in peraluminous granites generally have low grossular contents, unlike garnets from the Svarthopen and related hybrids.

Ca-rich garnet phenocrysts have been described from andesitic and dacitic rocks (Dawes and Evans, 1991; Green, 1992; Barnes and Allen, 2006), and in all cases the garnet phenocrysts were interpreted to have formed at pressures greater than 800 MPa. Therefore, the fact that garnets in Svarthopen area hybrids are distinct from those in regional migmatites and peraluminous granites, and the lack of garnets in otherwise similar mafic plutonic rocks in the region raise the question: what features of magma mixing in the Svarthopen pluton and similar hybrids resulted in garnet formation?

Conditions of Hybridization

On the basis of previous study of the Velfjord plutons (Barnes and Prestvik, 2000; Yoshinobu et al., 2002), we estimate the pressure of magma emplacement to be 600–700 MPa. This pressure range is identical to the pressure estimate from the garnet-hornblende-plagioclase thermobarometer (Kohn and Spear, 1990) discussed already. It is probable that the mafic magmas were relatively rich in H_2O, because the quartz gabbro and diorite samples contain primary poikilitic amphibole. The magmatic temperatures of possible end members at the time of mixing are difficult to

constrain. The Ti-in-zircon temperature estimate for granite sample N03.05 is ~750 °C, and the zircon saturation temperature is ~875 °C. Because this sample contains inherited zircon (Barnes et al., 2007), it is probable that the Ti-in-zircon temperature is the better estimate of the temperature of the granitic magmas at the time of magma mixing. The magmatic temperature of the mafic end member(s) cannot be measured because the primary pyroxenes have been replaced. An estimate of the temperature of a two-pyroxene– and plagioclase-saturated mafic end member was obtained using PELE (Boudreau, 1999) to model equilibrium crystallization of sample N87–48 with 3 wt% H_2O. At 700 MPa, the assemblage olivine, augite, orthopyroxene, and plagioclase (An_{80}) is stable at ~1020 °C. Plagioclase of An_{74} composition is stable at ~940 °C. Thus, we estimate that the temperature of the mafic end member was ≥940 °C.

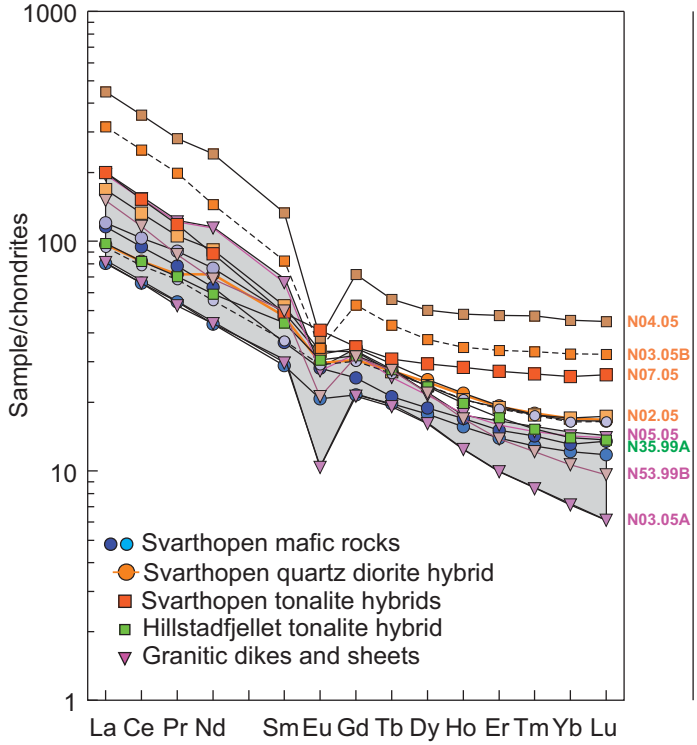

Figure 9. Rare earth element concentrations normalized to chondritic meteorites. Blue circles are compositions of diorite/quartz diorite samples; orange squares are compositions of garnet-bearing hybrids from the Svarthopen quarry, and green squares represent garnet-bearing hybrid from the eastern Hillstadfjellet pluton. Inverted triangles represent granitic rocks and the field of granite compositions is shown by gray shading.

Growth of Garnet and Effects of Metamorphism

The Kohn and Spear (1990) thermobarometer indicated equilibrium of garnet, amphibole, and plagioclase in the 500–550 °C range: amphibolite-facies conditions. This temperature range is consistent with the pervasive uralitization of pyroxene and with preservation of the primary amphibole + plagioclase assemblage in the gabbroic and dioritic rocks, because if ductile deformation had occurred at lower temperatures, both amphibole and intermediate plagioclase would have reacted to form greenschist-facies assemblages. Furthermore, several lines of evidence suggest that the Ca-rich garnet that typifies the hybrid rocks grew under magmatic conditions, rather than during metamorphism.

The distribution and size of the garnets in these rocks, the fact that biotite foliation is deflected around many garnets, and the fact that some garnets were sheared during high-temperature ductile deformation are all consistent with garnet growth above the solidus. Preservation of Ca-poor cores in some samples (e.g., N57.99A) indicates that some hybrids inherited garnet from granitic end-member magmas and that Ca-rich garnet mantled the inherited cores. Acicular apatite inclusions in Ca-rich garnets are also suggestive of garnet growth from a melt, or at least in a setting where magmatic acicular garnet was not recrystallized or deformed prior to garnet growth.

The Ca-rich compositions of garnets in the hybrids relative to the Ca-poor garnets in granitic rocks and regional migmatites indicate that the hybrid garnets are not inherited from a felsic end member or from host rocks. We tested the possibility that garnet could crystallize from a hybrid tonalitic magma using the program PELE (Boudreau, 1999). The composition of hybrid sample N57.99A was used with a range of H_2O contents between 0.4 and 1.5 wt%, fO_2 values of FMQ and FMQ+1, and pressure from 600 to 700 MPa. Calculated liquidus temperature varied between 1139 °C and 1155 °C. PELE provides two solution models for garnet, an ideal mixing model and the site-mixing model of Ganguly et al. (1996). Use of the latter model results in Ca- and Mg-rich garnet stable at the liquidus and crystallization of as much as 40% garnet by mass. Use of the former model results in garnet stability from ~700 °C to 750 °C, after crystallization of biotite and K-feldspar. In this model, garnet has low-Ca and low-Mg contents (~2.7% grossular, ~7.5% pyrope). Clearly, neither solution model matches the compositions of the natural garnets, but the Ganguly et al. (1996) model results in an unrealistically high temperature for garnet stability and an excessive mass of garnet crystallized, whereas the ideal mixing model results fit petrographic observations that garnet stability was well below the liquidus. We conclude that garnet growth at supersolidus temperatures was possible and that the lower calculated temperatures determined from garnet-amphibole thermobarometry represent equilibration during slow cooling.

The hybrid rocks are either peraluminous or are near the peraluminous-metaluminous boundary (Fig. 7E) and straddle the magnesian-ferroan boundary (Fig. 7C). By analogy with pelitic rocks, we suggest that magmatic garnets are restricted to these hybrid rock compositions specifically because of their relatively Fe-rich and peraluminous nature compared to other mafic and intermediate plutons in the region. It is possible that bulk composition of the hybrids is also responsible for the higher Ca contents of the garnets, compared to low-Ca garnets formed in granites (CaO < 4 wt%) and metapelitic rocks (CaO < 2 wt%; Barnes et al., 2002).

Mixing End Members

Identification of possible mixing end members is complicated by the fact that none of the analyzed rocks perfectly characterizes end members (Figs. 7 and 8). For the major-element data,

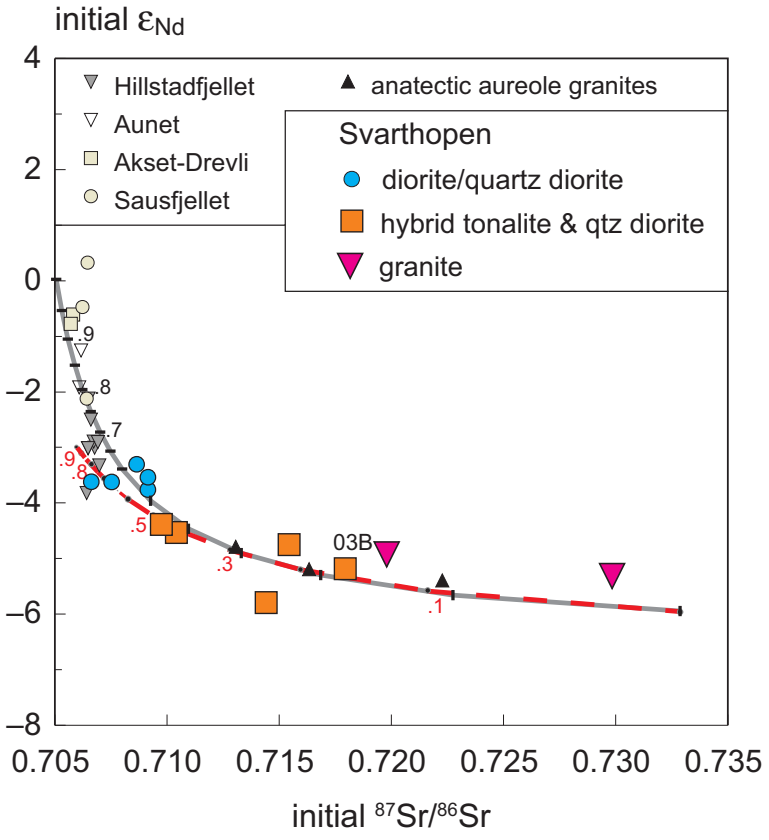

Figure 10. Nd and Sr isotope data for the Svarthopen pluton and nearby Velfjord plutons (Hillstadfjellet, Aunet, Akset-Drevli, and Sausfjellet). Two mixing curves are shown. The gray curve has a mafic end member (38 ppm Nd and ε_{Nd} = 0; 600 ppm Sr and initial $^{87}Sr/^{86}Sr$ = 0.7055) and a felsic end member (75 ppm Nd and ε_{Nd} = –6; 100 ppm Sr and initial $^{87}Sr/^{86}Sr$ = 0.735). The red mixing curve has a mafic end member (38 ppm Nd and ε_{Nd} = –3; 550 ppm Sr and initial $^{87}Sr/^{86}Sr$ = 0.706) and a felsic end member (26 ppm Nd and ε_{Nd} = –6; 72 ppm Sr and initial $^{87}Sr/^{86}Sr$ = 0.735). Tick marks on the two mixing curves indicate the proportion of the mafic end member.

it is possible to choose a SiO_2-poor dioritic composition (e.g., N87–48) and a granitic composition (e.g., N03.05A or N05.05) between which many of the hybrids plot. However, for several trace elements (e.g., Zr, Ba, REEs) (Fig. 6), concentrations increase from mafic compositions through the intermediate (hybrid) rocks and are lower among the granites (Figs. 8 and 9).

The patterns of Zr, Ba, and REE enrichment from dioritic through the tonalitic rocks may be explained in a number of ways: (1) The tonalitic rocks are not hybrids. This explanation may be correct, but the field relationships described previously herein and the smooth variation of Nd and Sr isotopes (Fig. 10) would then be quite fortuitous. (2) The felsic end member involved in mixing was granitic in composition but was not sampled or analyzed. If this is the case, then such a granitic end member would have trace-element abundances similar to A-type granites, with low Sr, and high Ba (~1000 ppm), Zr (~500 ppm), and Y (>80 ppm), and very high REE concentrations. To our knowledge, no such granite has been reported from the region. (3) The felsic end member was intermediate in composition. Sample 03.05B (Supplemental Table 4 [see footnote 4]; Figs. 7, 8, and 10) has ~65.5% SiO_2, plots at the silica-rich end of the array of garnet-bearing "hybrids," has the highest initial $^{87}Sr/^{86}Sr$ of the hybrid rocks, and has trace-element concentrations appropriate for a mixing end member. (4) Hybridization was not a simple mixing process and involved fractional crystallization and local crystal accumulation. In the field, modal heterogeneity in the hybrid zones is evident (Fig. 2), and this heterogeneity is reflected in geochemical compositions. For example, samples N55.99C and N07.05 have higher abundances of Al_2O_3, CaO, and Na_2O than the main array of Svarthopen rocks. These anomalously high values may be explained by accumulation of plagioclase. High abundances of Sr and the lack of a Eu anomaly for sample N07.05 (Fig. 9) are consistent with this interpretation. In contrast, the variation of Y and REE abundances from diorite through tonalite cannot be explained by accumulation of garnet because even if garnet were a magmatic phase, it was only stable near the solidus. Zircon accumulation is also thought to be unlikely to cause the overall increase in Zr abundance from dioritic to tonalitic rocks; however, zircon accumulation can probably explain the high Zr abundances in the four samples that plot above the trend in Figure 8D.

Instead of crystal accumulation, we suggest that increasing abundances of Zr and REEs (and Ba) from dioritic to tonalitic compositions were the result of initial magma mixing followed by fractional crystallization of the hybrid magmas. In this model, we envision magma mixing to have resulted in a range of hybrid magmas that individually underwent fractional crystallization of plagioclase + pyroxenes, thereby enriching the residual magmas in incompatible elements. This process can explain the lack of correlation between initial $^{87}Sr/^{86}Sr$ and either Zr or LREEs, because although mixing would control the value of initial $^{87}Sr/^{86}Sr$ and would result in a general correlation of initial $^{87}Sr/^{86}Sr$ with SiO_2, post-mixing fractionation within individual magma batches would result in variable, nonuniform abundances of the incompatible elements such as Zr and the LREEs (Figs. 8D and 9).

Trace-element compositions of garnet can help provide details of this process. The REE patterns of garnets from the hybrid tonalites have shapes that range from typical magmatic garnet patterns (e.g., cores in garnet from N57.99A; Fig. 5D) to ones with nearly flat HREE slopes (e.g., N132.00; Fig. 5E). The garnet patterns with low HREE abundances are similar to those of garnets associated with hydrothermal vent systems in the Broken Hill region of Australia (Heimann et al., 2011). The garnets in the hybrid tonalites are similar in bulk composition to some hydrothermal garnets, although the hydrothermal garnets range to higher spessartine contents and occur in garnet-rich assemblages (many are garnetites) that contain quartz, micas, grunerite, gahnite, and magnetite (Heimann et al., 2011). Heimann et al. (2011) interpreted the flat HREE patterns of the hydrothermal garnets to reflect the bulk composition of the rock in which the garnets grew.

An origin of the garnets in the hybrid rocks by hydrothermal processes seems unlikely because of the textural evidence cited previously, because of the widely dispersed nature of the garnets (in

hand specimen to outcrop scale), and because of the lack of evidence for hydrothermal exchange elsewhere in the Svarthopen or other garnet-bearing units. What then explains the REE patterns of garnets from hybrid rocks compared to typical patterns of magmatic garnets? If the garnets from the hybrids grew at near-solidus conditions, then the residual melt would have undergone fractionation of zircon, apatite, and allanite, and possibly xenotime. Therefore, Zr would have been sequestered in zircon, HREEs in zircon and xenotime, and LREEs in allanite, resulting in the observed REE patterns and low Zr contents in garnets from hybrid rocks (Fig. 6).

Consequences of Garnet Formation in Ferroan, Peraluminous Hybrids

In the Svarthopen and related garnet-bearing plutonic units of the Velfjord area, mixing of metaluminous mafic magmas with peraluminous felsic magmas has yielded suites of rocks having compositions that straddle the metaluminous-peraluminous and magnesian-ferroan boundaries. We suggest that these hybrid magmas had compositions in which garnet was stable under middle-crustal conditions. It is generally accepted that garnet is a common phase in pelitic (peraluminous) migmatites but that garnet stability requires pressures >1.0 GPa in mafic rocks and magmas (Wolf and Wyllie, 1993, 1994; Rapp and Watson, 1995). If magma hybridization is as common in the lower crust as generally postulated, and if felsic end members in the lower crust are peraluminous, then it follows that in some instances the hybrid magmas will crystallize garnet. In fact, if the mafic end member underwent fractional crystallization along an iron enrichment trend prior to mixing, as would be expected in relatively low-fO_2 magmas, then mixing of an Fe-rich mafic magma with peraluminous felsic end members should result in Fe- and Al-rich hybrids in which significant garnet growth is possible at pressures typical of lower-crustal conditions (Fig. 11). If garnet is stabilized during lower-crustal magma mixing, then it is likely that high-pressure differentiation of the hybrid magmas will involve fractionation of garnet and result in differentiates with low HREE and Y contents. If the Svarthopen example may be used, the differentiated magmas would not necessarily display uniform trace-element trends, owing to differences in the proportion of mixing end members. In effect, lower-crustal mixing followed by fractional crystallization could produce suites of magmas with a range of isotopic values and lacking smooth compositional trends, which would be interpreted as products of crustal melting of a heterogeneous source. For example, the most felsic garnet-bearing Svarthopen hybrids lack amphibole and could be interpreted to be partial melts of metagraywacke protoliths, whereas intermediate Svarthopen hybrids contain garnet and amphibole and could be interpreted to be partial melts of potassic garnet amphibolite protoliths.

Whether or not postmixing fractional crystallization occurred, the solid products of deep-crustal hybridization would mirror the heterogeneities inherent in the lower crust or in melts derived from lower-crustal rocks. Partial melting of these heterogeneous, lower-crustal hybrids would probably begin with biotite-dehydration melting reactions, resulting in relatively high-temperature, K-rich partial melts (e.g., Vielzeuf and Montel, 1994; Patiño Douce, 1999). Such melting would result in residual garnet, which, when combined with garnet already present due to mixing, would impose a steep, negative slope on the REE pattern of the melt.

If hybrid source rocks contained low Sr and high Ba, Y, and Zr, as seen in the Svarthopen hybrids, the resulting magmas would share many features with so-called potassic A-type granites. An example of one such pluton is the 439 Ma Heilhornet pluton (Nordgulen and Schouenborg, 1990; Barnes et al., 2007), which is alkali-calcic, mainly ferroan, or transitional magnesian-ferroan, has K_2O contents around 5 wt%, and has high contents of Zr and Nb and low contents of Sr compared to most Bindal Batholith plutons (e.g., Nordgulen, 1993). It is noteworthy that the Heilhornet pluton contains inherited zircons for which ages range from 462 to 471 Ma—a range of ages that encompasses emplacement of the Svarthopen pluton.

Several studies have documented evidence for hybridization of mafic magmas with lower-crustal rocks/magmas (e.g., Hildreth and Moorbath, 1988; Williams et al., 1995; Voshage et al., 1990; Koteas et al., 2010; Jagoutz et al., 2011). In some cases, Moho-depth magmatism has resulted in formation of dense, garnet-bearing cumulates. For example, Ducea and Saleeby (1998) and Saleeby et al. (2003) showed that dense, garnet-bearing (eclogitic) roots of thick (80 km) Sierra Nevada arc crust were delaminated during Tertiary time. The results of this study suggest that garnet productivity in the lower crust may be enhanced if mixing occurs between Fe-rich differentiates and peraluminous crustal melts. Such conditions can be expected in hot-zone environments (e.g., Annen et al., 2006). If this is the case, then it is conceivable that significant masses of garnet-rich hybrids could form and delaminate from the base of arc crust of average (e.g., 40 km) thickness.

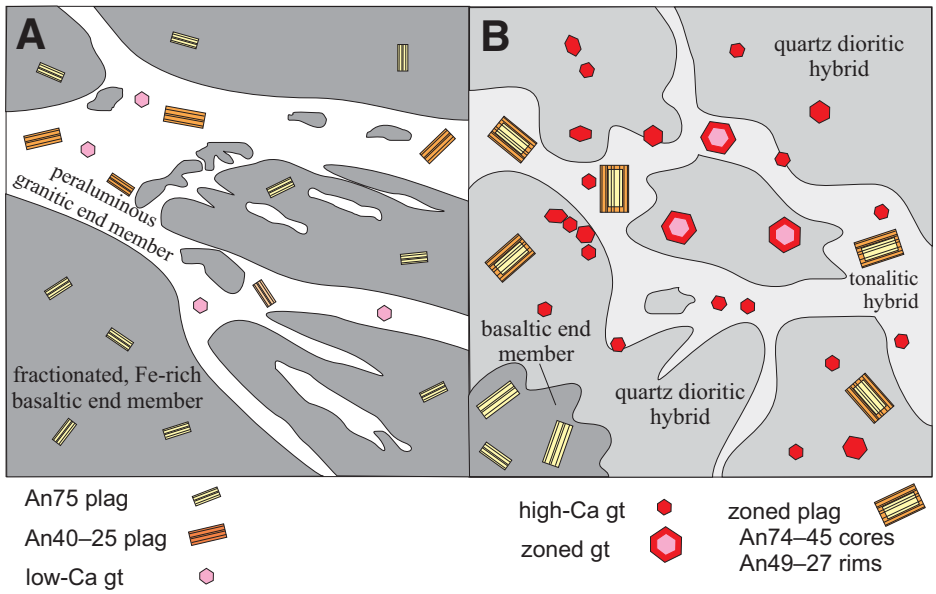

Figure 11. Cartoon illustrating changes in mineral compositions caused by mixing. (A) Incipient mingling of a basaltic end member with calcic plagioclase and a granitic end member that contains phenocrysts of intermediate plagioclase and Ca-poor almandine garnet. (B) Results of hybridization. Quartz dioritic and tonalitic hybrids represent differing end-member proportions. Most garnet is Ca rich, but locally garnets have Ca-poor cores similar to garnet in the granitic end member. Plagioclase crystals have a distinct zonal boundary between calcic-to-intermediate, normally zoned cores and intermediate-to-sodic, normally zoned rims.

CONCLUSIONS

Garnet-bearing tonalitic rocks in the Svarthopen pluton formed during mixing of dioritic and granitic magmas in a middle-crustal setting. Textural data are permissive of garnet growth from a melt at conditions near the solidus. The hybrid magmas underwent fractional crystallization after mixing and prior to garnet crystallization, such that incompatible element concentrations in hybrid rocks do not lie on mixing arrays but Nd and Sr isotope ratios do. Enrichment of Zr and the REEs during postmixing fractional crystallization resulted in precipitation of zircon, allanite, and xenotime (?) prior to garnet crystallization. Stability of these accessory phases resulted in distinctly low REE and Zr abundances and relatively flat HREE patterns in the garnets.

Middle-crustal mixing in the Svarthopen magma system combined peraluminous, ferroan magmas with metaluminous, magnesian ones. In deep-crustal settings, such mixing should be widespread, particularly in continental arcs and zones of continental collision, where pelitic metasedimentary rocks may be deeply buried and melted. In the deep crust, postmixing fractionation of hybrid magmas could greatly increase the diversity of major- and trace-element abundances, yet leave the isotopic signature of mixing intact, complicating any interpretation concerning the sources and processes responsible for formation of granitic magmas in MASH/hot-zone environments. Finally, if sufficient volumes of garnet-rich hybrid rocks form in the deep crust, then it is possible that these hybrids will founder into the upper mantle. As the foundered hybrids physically mix with mantle rocks, they will impart a crustal geochemical signature to the mantle—a signature that could then be imparted to mafic magmas formed by later mantle melting.

ACKNOWLEDGMENTS

We thank Melanie Barnes for assistance in the field and laboratory, and Susan Swapp for assistance with microprobe analyses. The manuscript benefited greatly from reviews by Jade Star Lackey, Matt Rioux, and Jeff Amato. This research was supported by National Science Foundation grants EAR-9814280 and EAR-0439750 and by the Norwegian Geological Survey.

REFERENCES CITED

Allan, B.D., and Clarke, D.B., 1981, Occurrence and origin of garnets in the South Mountain batholith, Nova Scotia: Canadian Mineralogist, v. 19, p. 19–24.

Anderson, H.A., Yoshinobu, A.S., and Chamberlain, K., 2007, Xenolith incorporation in plutons: Implications to stoping, assimilation, and incremental pluton construction, Andalshatten pluton, Norwegian Caledonides: Geological Society of America Abstracts with Programs, v. 39, no. 6, p. 225.

Annen, C., Blundy, J.D., and Sparks, R.S.J., 2006, The genesis of intermediate and silicic magmas in deep crustal hot zones: Journal of Petrology, v. 47, p. 505–539, doi:10.1093/petrology/egi084.

Barnes, C.G., and Allen, C.M., 2006, Depth of origin of late Middle Jurassic garnet andesite, southern Klamath Mountains, *in* Snoke, A.W., and Barnes, C.G., eds., Geological Studies in the Klamath Mountains Province, California and Oregon: A Volume in Honor of William P. Irwin: Geological Society of America Special Paper 410, p. 269–286.

Barnes, C.G., and Prestvik, T., 2000, Conditions of pluton emplacement and anatexis in the Caledonian Bindal Batholith, north-central Norway: Norsk Geologisk Tidsskrift, v. 80, p. 259–274, doi:10.1080/00291960051030581.

Barnes, C.G., Prestvik, T., Nordgulen, Ø., and Barnes, M.A., 1992, Geology of three dioritic plutons in Velfjord, Nordland: Norges Geologiske Undersøkelse Bulletin, v. 423, p. 41–54.

Barnes, C.G., Yoshinobu, A.S., Prestvik, T., Nordgulen, Ø., Karlsson, H.R., and Sundvoll, B., 2002, Mafic magma intraplating: Anatexis and hybridization in arc crust, Bindal Batholith, Norway: Journal of Petrology, v. 43, p. 2171–2190, doi:10.1093/petrology/43.12.2171.

Barnes, C.G., Dumond, G., Yoshinobu, A.S., and Prestvik, T., 2004, Assimilation and crystal accumulation in a mid-crustal magma chamber: The Sausfjellet pluton, north-central Norway: Lithos, v. 75, p. 389–412, doi:10.1016/j.lithos.2004.04.036.

Barnes, C.G., Prestvik, T., Sundvoll, B., and Surratt, D., 2005, Pervasive assimilation of carbonate and silicate rocks in the Hortavær igneous complex, north-central Norway: Lithos, v. 80, p. 179–199, doi:10.1016/j.lithos.2003.11.002.

Barnes, C.G., Frost, C.D., Yoshinobu, A., McArthur, K., Barnes, M.A., Allen, C.M., Nordgulen, Ø., and Prestvik, T., 2007, Timing of sedimentation, metamorphism, and plutonism in the Helgeland Nappe Complex, north-central Norwegian Caledonides: Geosphere, v. 3, p. 683–703, doi:10.1130/GES00138.1.

Barnes, C.G., Reid, K., Frost, C.D., Barnes, M.A., Allen, C.M., and Yoshinobu, A.S., 2011, Ordovician and Silurian magmatism in the Upper Nappe, Uppermost Allochthon, Helgeland Nappe Complex, north-central Norway: Norwegian Journal of Geology, v. 91, p. 121–136.

Beard, J.S., and Lofgren, G.E., 1991, Dehydration melting and water-saturated melting of basaltic and andesitic greenstones and amphibolites at 1, 3, and 6.9 kb: Journal of Petrology, v. 32, p. 365–401.

Birkeland, A., Nordgulen, Ø., Cumming, G.L., and Bjørlykke, A., 1993, Pb-Nd-Sr isotopic constraints on the origin of the Caledonian Bindal Batholith, central Norway: Lithos, v. 29, p. 257–271, doi:10.1016/0024-4937(93)90020-D.

Boudreau, A.E., 1999, PELE—A version of the MELTS software program for the PC platform: Computers & Geosciences, v. 25, p. 201–203, doi:10.1016/S0098-3004(98)00117-4.

Clemens, J.D., Holloway, J.R., and White, A.J.R., 1986, Origin of an A-type granite: Experimental constraints: The American Mineralogist, v. 71, p. 317–324.

Collins, W.J., 1994, Upper- and middle-crustal response to delamination: An example from the Lachlan fold belt, eastern Australia: Geology, v. 22, p. 143–146, doi:10.1130/0091-7613(1994)022<0143:UAMCRT>2.3.CO;2.

Dawes, R.L., and Evans, B.W., 1991, Mineralogy and geothermobarometry of magmatic epidote-bearing dikes, Front Range, Colorado: Geological Society of America Bulletin, v. 103, p. 1017–1031, doi:10.1130/0016-7606(1991)103<1017:MAGOME>2.3.CO;2.

Ducea, M., and Saleeby, J., 1998, A case for delamination of the deep batholithic crust beneath the Sierra Nevada, California: International Geology Review, v. 40, p. 78–93, doi:10.1080/00206819809465199.

Dufek, J., and Bergantz, G.W., 2005, Lower crustal magma genesis and preservation: A stochastic framework for the evaluation of basalt–crust interaction: Journal of Petrology, v. 46, p. 2167–2195.

Erdmann, S., Jamieson, R.A., and Macdonald, M.A., 2009, Evaluation the origin of garnet, cordierite, and biotite in granitic rocks: A case study from the South Mountain Batholith, Nova Scotia: Journal of Petrology, v. 50, p. 1477–1503, doi:10.1093/petrology/egp038.

Farmer, G., Glazner, A., and Manley, C., 2002, Did lithospheric delamination trigger late Cenozoic potassic volcanism in the southern Sierra Nevada, California?: Geological Society of America Bulletin, v. 114, p. 754–768, doi:10.1130/0016-7606(2002)114<0754:DLDTLC>2.0.CO;2.

Ferry, J.M., and Watson, E.B., 2007, New thermodynamic models and revised calibrations for the Ti-in-zircon and Zr-in-rutile thermometers: Contributions to Mineralogy and Petrology, v. 154, p. 429–437, doi:10.1007/s00410-007-0201-0.

Frost, B.R., and Frost, C.D., 2008, A geochemical classification for feldspathic igneous rocks: Journal of Petrology, v. 49, p. 1955–1969, doi:10.1093/petrology/egn054.

Frost, B.R., Barnes, C.G., Collins, W.J., Arculus, R.J., Ellis, D.J., and Frost, C.D., 2001, A geochemical classification for granitic rocks: Journal of Petrology, v. 42, p. 2033–2048, doi:10.1093/petrology/42.11.2033.

Ganguly, J., Cheng, W., and Tirone, M., 1996, Thermodynamics of aluminosilicate garnet solid solution: New experimental data, an optimized model, and thermometric applications: Contributions to Mineralogy and Petrology, v. 126, p. 137–151, doi:10.1007/s004100050240.

Green, T.H., 1992, Experimental phase equilibrium studies of garnet-bearing I-type volcanics and high-level intrusives from Northland, New Zealand: Transactions of the Royal Society of Edinburgh–Earth Sciences, v. 83, p. 429–438, doi:10.1017/S0263593300008105.

Gustavoson, M., and Prestvik, T., 1979, The igneous complex of Hortavær, Nord-Trøndelag, central Norway: Norges geologiske undersøkelse Bulletin, v. 348, p. 73–92.

Heimann, A., Spry, P.G., Teale, G.S., Conor, C.H.H., and Pearson, N.J., 2011, The composition of garnet in garnet-rich rocks in the southern Proterozoic Curnamona Province, Australia: An indicator of the premetamorphic physicochemical conditions of formation: Mineralogy and Petrology, v. 101, p. 49–74, doi:10.1007/s00710-010-0130-x.

Hildreth, W., and Moorbath, S., 1988, Crustal contributions to arc magmatism in the Andes of central Chile: Contributions to Mineralogy and Petrology, v. 98, p. 455–489, doi:10.1007/BF00372365.

Jagoutz, O., Müntener, O., Schmidt, M.W., and Burg, J.-P., 2011, The roles of flux- and decompression melting and their respective fractionation lines for continental crust formation: Evidence from the Kohistan arc: Earth and Planetary Science Letters, v. 303, p. 25–36, doi:10.1016/j.epsl.2010.12.017.

Kohn, M.J., and Spear, F.S., 1990, Two new geobarometers for garnet amphibolites, with applications to southeastern Vermont: The American Mineralogist, v. 75, p. 89–96.

Koteas, G.C., Williams, M.L., Seaman, S.J., and Dumond, G., 2010, Granite genesis and mafic-felsic magma interaction in the lower crust: Geology, v. 38, p. 1067–1070, doi:10.1130/G31017.1.

Lackey, J.S., Erdmann, S., Hark, J.S., Nowak, R.M., Murray, K.E., Clarke, D.B., and Valley, J.W., 2011, Tracing garnet origins in granitoid rocks by oxygen isotope analysis: Examples from the South Mountain Batholith, Nova Scotia: Canadian Mineralogist, v. 49, p. 417–439, doi:10.3749/canmin.49.2.417.

Leake, B., et al., 1997, Nomenclature of amphiboles: Report of the Subcommittee on Amphiboles of the International Mineralogical Association, Commission on New Minerals and Mineral Names: Canadian Mineralogist, v. 35, p. 219–246.

Lee, C.-T.A., Cheng, X., and Horodyskyj, U., 2006, The development and refinement of continental arcs by primary basaltic magmatism, garnet pyroxenite accumulation, basaltic recharge and delamination: Insights from the Sierra Nevada, California: Contributions to Mineralogy and Petrology, v. 151, p. 222–242, doi:10.1007/s00410-005-0056-1.

Lustrino, M., 2005, How the delamination and detachment of lower crust can influence basaltic magmatism:

Earth-Science Reviews, v. 72, p. 21–38, doi:10.1016/j.earscirev.2005.03.004.

Miller, C.F., and Stoddard, E.F., 1981, The role of manganese in the paragenesis of magmatic garnet: An example from the Old Woman–Piute Range, California: The Journal of Geology, v. 89, p. 233–246, doi:10.1086/628582.

Mori, L., Gómez-Tuena, A., Schaaf, P., Goldstein, S.L., Pérez-Arvizu, O., and Solís-Pichardo, G., 2009, Lithospheric removal as a trigger for flood basalt magmatism in the Trans-Mexican volcanic belt: Journal of Petrology, v. 50, p. 2157–2186, doi:10.1093/petrology/egp072.

Myrland, R., 1972, Velfjord: Beskrivelse til det Berggrunns: Norges Geologiske Undersøkelse Geologiske Gradteigskart I 18, oversize map sheet, scale 1:100,000.

Nissen, A.L., Roberts, D., and Gromet, L.P., 2006, U-Pb zircon ages of a tonalite and a granodiorite dyke from the southeastern part of the Bindal Batholith, central Norwegian Caledonides: Norges Geologiske Undersøkelse Bulletin, v. 446, p. 5–9.

Nordgulen, Ø., 1993, A Summary of the Petrography and Geochemistry of the Bindal Batholith: Geological Survey of Norway Report 92.111, 103 p.

Nordgulen, Ø., and Schouenborg, B., 1990, The Caledonian Heilhornet pluton, north-central Norway: Geological setting, radiometric age and implications for the Scandinavian Caledonides: Journal of the Geological Society of London, v. 147, p. 439–450, doi:10.1144/gsjgs.147.3.0439.

Nordgulen, Ø., and Sundvoll, B., 1992, Strontium isotope composition of the Bindal Batholith, Central Norwegian Caledonides: Norges Geologiske Undersøkelse Bulletin, v. 423, p. 19–39.

Nordgulen, Ø., Bickford, M.E., Nissen, A.L., and Wortman, G.L., 1993, U-Pb zircon ages from the Bindal Batholith, and the tectonic history of the Helgeland Nappe Complex, Scandinavian Caledonides: Journal of the Geological Society of London, v. 150, p. 771–783, doi:10.1144/gsjgs.150.4.0771.

Patiño Douce, A.E., 1999, What do experiments tell us about the relative contributions of crust and mantle to the origin of granitic magmas?, *in* Castro, A., Fernandez, C., and Vigneresse, J., eds., Understanding Granites: Integrating New and Classical Techniques: London, Geological Society of London, p. 55–75.

Patiño Douce, A.E., and Johnston, A.D., 1991, Phase equilibria and melt productivity in the pelitic system: Implications for the origin of peraluminous granitoids and aluminous granulites: Contributions to Mineralogy and Petrology, v. 107, p. 202–218, doi:10.1007/BF00310707.

Rapp, R.P., and Watson, E.B., 1995, Dehydration melting of metabasalt at 8–32 kbar: Implications for continental growth and crust-mantle recycling: Journal of Petrology, v. 36, p. 891–931.

Roberts, D., 2003, The Scandinavian Caledonides: Event chronology, palaeogeographic settings and likely modern analogues: Tectonophysics, v. 365, p. 283–299, doi:10.1016/S0040-1951(03)00026-X.

Saleeby, J., Ducea, M., and Clemens-Knott, D., 2003, Production and loss of high-density batholithic root, southern Sierra Nevada, California: Tectonics, v. 22, doi:10.1029/2002TC001374.

Skjerlie, K.P., and Johnston, A.D., 1992, Vapor-absent melting at 10 kbar of a biotite- and amphibole-bearing tonalitic gneiss: Implications for the generation of A-type granites: Geology, v. 20, p. 263–266, doi:10.1130/0091-7613(1992)020<0263:VAMAKO>2.3.CO;2.

Skjerlie, K.P., and Johnston, A.D., 1996, Vapour-absent melting from 10 to 20 kbar of crustal rocks that contain multiple hydrous phases: Implications for anatexis in the deep to very deep continental crust and active continental margins: Journal of Petrology, v. 37, p. 661–691, doi:10.1093/petrology/37.3.661.

Stephens, M., and Gee, D., 1989, Terranes and polyphase accretionary history in the Scandinavian Caledonides, *in* Dallmeyer, R.D., ed., Terranes in the Circum-Atlantic Paleozoic Orogens: Geological Society of America Special Paper 230, p. 17–30.

Stephens, M.B., Gustavson, M., Ramberg, I.B., and Zachrisson, E., 1985, The Caledonides of central-north Scandinavia—A tectonostratigraphic overview, *in* Gee, D.G., and Sturt, B.A., eds., The Caledonide Orogen—Scandinavia and Related Areas: Chicester, John Wiley and Sons Ltd., p. 135–162.

Thorsnes, T., and Løseth, H., 1991, Tectonostratigraphy in the Velfjord-Tosen region, southwestern part of the Helgeland Nappe Complex, central Norwegian Caledonides: Norges Geologiske Undersøkelse Bulletin, v. 421, p. 1–18.

Vernon, R.H., 1983, Restite, xenoliths and microgranitoid enclaves in granites: Journal and Proceedings: Royal Society of New South Wales, v. 116, p. 77–103.

Vielzeuf, D., and Montel, J.M., 1994, Partial melting of metagreywackes. Part I. Fluid-absent experiments and phase relationships: Contributions to Mineralogy and Petrology, v. 117, p. 375–393, doi:10.1007/BF00307272.

Voshage, H., Hofmann, A.W., Mazzucchelli, M., Rivalenti, G., Sinigoi, S., Raczek, I., and Demarchi, G., 1990, Isotopic evidence from the Ivrea zone for a hybrid lower crust formed by magmatic underplating: Nature, v. 347, p. 731–736, doi:10.1038/347731a0.

Watson, E.B., Wark, D.A., and Thomas, J.B., 2006, Crystallization thermometers for zircon and rutile: Contributions to Mineralogy and Petrology, v. 151, p. 413–433, doi:10.1007/s00410-006-0068-5.

Wells, M.L., and Hoisch, T.D., 2008, The role of mantle delamination in widespread Late Cretaceous extension and magmatism in the Cordilleran orogen, western United States: Geological Society of America Bulletin, v. 120, p. 515–530, doi:10.1130/B26006.1.

Williams, M.L., Hanmer, S., Kopf, C., and Darrach, M., 1995, Syntectonic generation and segregation of tonalitic melts from amphibolite dikes in the lower crust, Striding-Athabasca mylonite zone, northern Saskatchewan: Journal of Geophysical Research, v. 100, p. 15,717–15, 734.

Wolf, M.B., and Wyllie, P.J., 1993, Garnet growth during amphibolite anatexis: Implications of a garnetiferous restite: The Journal of Geology, v. 101, p. 357–373, doi:10.1086/648229.

Wolf, M.B., and Wyllie, P.J., 1994, Dehydration-melting of amphibolite at 10 kbar: The effects of temperature and time: Contributions to Mineralogy and Petrology, v. 115, p. 369–383, doi:10.1007/BF00320972.

Xu, J.-F., Shinjo, R., Defant, M., Wang, Q., and Rapp, R., 2002, Origin of Mesozoic adakitic intrusive rocks in the Ningzhen area of east China: Partial melting of delaminated lower continental crust?: Geology, v. 30, p. 1111–1114, doi:10.1130/0091-7613(2002)030<1111:OOMAIR>2.0.CO;2.

Yoshinobu, A.S., Barnes, C.G., Nordgulen, Ø., Prestvik, T., Fanning, M., and Pedersen, R.B., 2002, Ordovician magmatism, deformation, and exhumation in the Caledonides of central Norway: An orphan of the Taconic orogeny?: Geology, v. 30, p. 883–886, doi:10.1130/0091-7613(2002)030<0883:OMDAEI>2.0.CO;2.

Zen, E.-A., 1988, Phase relations of peraluminous granitic rocks and their petrogenetic implications: Annual Review of Earth and Planetary Sciences, v. 16, p. 21–51, doi:10.1146/annurev.ea.16.050188.000321.

Zhang, C., Ma, C., and Holtz, F., 2010, Origin of high-Mg adakitic magmatic enclaves from the Meichuan pluton, southern Dabie orogen (central China): Implications for delamination of the lower continental crust and melt-mantle interaction: Lithos, v. 119, p. 467–484, doi:10.1016/j.lithos.2010.08.001.

Manuscript Received 16 June 2011
Revised Manuscript Received 26 December 2011
Manuscript Accepted 31 December 2011